## Analyzing density-driven errors: Principles and pitfalls

SEHUN KIM<sup>a</sup>, DO-GYEONG LEE<sup>a</sup>, GYUMIN KIM<sup>a</sup>, YOUNGSAM KIM<sup>a</sup>, MIHIRA SOGAL<sup>b</sup>, STEVEN CRISOSTOMO<sup>c</sup>, KIERON BURKE<sup>b,c</sup>, AND EUNJI SIM<sup>a\*</sup>

<sup>a</sup>Department of Chemistry, Yonsei University, 50 Yonsei-ro Seodaemun-gu, Seoul 03722, Korea.

<sup>b</sup>Department of Physics and Astronomy, University of California, Irvine, CA 92697, USA

<sup>c</sup>Department of Chemistry, University of California, Irvine, CA 92697, USA

September 22, 2025

#### Abstract

The theory of density-corrected density functional theory (DC-DFT) separates the error in any approximate DFT calculation into a functional-driven contribution and a density-driven error. Practical DC-DFT calculations often use the Hartree-Fock density instead of a self-consistent DFT density—a method known as HF-DFT—and reduce energetic errors in several classes of chemical problems. Using principles of DC-DFT, we illustrate several pitfalls when analyzing HF-DFT errors, including an interpolator for density-driven errors that is chronically inaccurate, using proxies instead of accurate densities, and conflating common measures of density errors with those of DC-DFT. We report ideal density-driven errors for one- and two-electron systems, where we can calculate most properties exactly, illustrating these problems. A simple analysis of benchmarking data shows that proxy densities proposed in recent literature are too inaccurate to be useful in DC-DFT. Despite recent claims to the contrary, we show that the success of DC-DFT for barrier heights does not rely on a cancellation of errors, and it is to be expected that HF-DFT errors can be smaller than functional errors, but we fall short of explaining why the improvement is so quantitatively systematic.

## I. Introduction

Kohn-Sham Density Functional Theory (KS-DFT)<sup>1</sup> is a widely used approach in computational chemistry due to its balance of accuracy and computational efficiency. Density-corrected DFT (DC-DFT)<sup>2</sup> is a general methodology for separating errors in any DFT calculation into two well-defined contributions: a functional error and a density-driven error. Most DFT errors are dominated by functional errors, so the density does not matter. But many specific classes of DFT calculations have been found to have significant density-driven errors. In such cases, the simple expedient of using the Hartree-Fock (HF)<sup>3</sup> density in place of the self-consistent DFT density-referred to as HF-DFT-often reduces the error, sometimes quite substantially. In fact, the overall performance of the weighted total mean absolute deviation (WTMAD-2) measure of error on the GMTKN55<sup>4</sup> database (general-main group thermochemistry, kinetics, and noncovalent interactions) of many standard functionals is significantly improved by use of HF densities <sup>5–9</sup>, when the principles of DC-DFT are applied judiciously.

Such practical successes should not obscure the generality and power of DC-DFT analysis. DC-DFT does not rely on HF densities. It applies to every self-consistent KS calculation ever run. It provides a singular measure of density error that uniquely quantifies the error in terms of its energetic

consequences (if errors in densities have negligible energetic consequences, why worry about them?). Density-driven errors overlap with, but are not identical to, delocalization errors.

After all, stretched  $H_2^+$  is the prototype self-interaction error,  $^{10}$  but those are functional-driven errors for standard semilocal approximations, not density-driven. The prototypical density-driven error is anions, where a truly self-consistent KS calculation with a semilocal approximation typically loses about 0.3 electrons.  $^{11}$ 

Here, the functional error refers to the numerical deviation obtained by evaluating the approximate functional on the exact density, whereas the density-driven error denotes the error arising from the use of the approximate density. The density error quantifies the deviation of the approximate density itself from the exact density, and the functional-driven error more broadly describes the intrinsic inaccuracy of the approximate functional.

The obvious explanation for the success of DC-DFT using HF densities in density-sensitive problems is that (a) the HF density is physically more sound and much closer to the exact density than the self-consistent DFT density, and (b) the removal of density-driven errors substantially reduces the overall error. This behavior has been demonstrated in several simple cases. <sup>12</sup> However, several recent papers <sup>13–16</sup> have questioned this explanation, especially in the high-profile case

<sup>\*</sup>esim@yonsei.ac.kr

of transition-state barriers, water clusters, and halogen and chalcogen complexes. These papers argue that the improved energy of HF-DFT is due to the use of an overlocalized HF density, which changes the sign of the density-driven error of the delocalized approximate functional, causing cancellation with the functional error. In particular, it would appear that the density-driven errors of HF densities are much greater than those of self-consistent densities. This has led to various speculations and explanations as to the source of the highly systematic error reductions in HF-DFT.

The current paper shows that these analyses are flawed, and so illustrates the importance of the exact theory of DC-DFT. We report the first calculations of *ideal* density-driven errors, for which the density-driven errors of DC-DFT are pragmatic approximations. These ideal density-driven errors are extremely difficult to calculate in general, but we have managed in a few one- and two-electron cases. These few examples demonstrate that density-driven errors on self-consistent densities are generally good approximations to ideal density-driven errors, but that the density-driven error interpolator, used in all the 'cancellation' papers, is entirely unreliable. There is no credible evidence that HF-DFT has larger density-driven errors than those of self-consistent densities. In these special cases, we can actually find the self-consistent density of an inconsistent evaluation, and show that it is better than the original self-consistent density.

Another bad habit that has crept into the literature is the use of proxy densities instead of accurate benchmark densities. We demonstrate that these are nowhere near accurate enough to usefully measure typical density-driven errors.

Lastly, we explain why there is little connection between the errors reported in DC-DFT and various 'natural' measures, such as  $L_2$  norms, both because DC-DFT is applied to energy differences, and because of the subtleties of using energy functionals to quantify density errors.

We use both the principles and the practical results of these calculations to analyze recent papers that suggest that HF-DFT relies on an unconventional cancellation of errors. Our analysis strongly suggests that the estimates of the density-driven error of HF-DFT are highly inaccurate and a gross overestimate. Because the density-driven error of HF-DFT (distinct from the HF density itself) is expected to be much smaller than the functional error, the observed accuracy cannot be attributed to any fortuitous error cancellation. From a DC-DFT perspective, we also provide an indirect explanation of why the HF density can yield a lower energy error than the exact density. Rumors of the death of DC-DFT appear to have been exaggerated.

### II. Background

## II1. Principles

Most ground-state electronic structure methods are primarily used to extract  $E_v$ , the ground-state energy as a functional of the one-body potential  $v(\mathbf{r})$ . Chemical reaction energies are the differences in energies for two different potentials. Derivatives with respect to nuclear positions determine forces, vibrations, and equilibrium geometries. Given its importance, almost all such methods have been tuned to optimize accuracy in energies. The Rayleigh-Ritz variational principle states  $^{17}$ :

$$E_v = \min_{\Psi} \langle \Psi | \hat{H}_v | \Psi \rangle \tag{1}$$

where the minimization is over all antisymmetric wavefunctions with N electrons, and  $\hat{H}_v$  is the electronic Hamiltonian. In fact, even the density can (in principle) be extracted directly from a sequence of such calculations via

$$n_v(\mathbf{r}) = \frac{\delta E_v}{\delta v(\mathbf{r})} \tag{2}$$

for a given N. A KS-DFT calculation writes the variational principle in terms of the density:

$$E_v = \min_n E_v[n] = E_v[n_v], \tag{3}$$

where the minimization is over all (Lieb-allowed  $^{18}$ ) densities integrating to  ${\cal N}$  and

$$E_v[n] = T_S[n] + U[n] + E_{XC}[n] + \int d^3r \ n(\mathbf{r}) v(\mathbf{r}). \tag{4}$$

Here  $T_{\rm S}$  is the KS kinetic energy, U the Hartree energy, and  $E_{\rm XC}$  is the exchange-correlation (XC) energy, which is approximated in practical calculations. The self-consistent solution of the KS equations performs precisely the minimization of Eq. 3. Moreover, at self-consistency, the KS density is exactly equal to that of Eq. 2, by construction. In reality, all modern DFT calculations are spin-density calculations  $^{19}$ , but we give formulas in terms of the total density for simplicity. We also use energy units of Hartrees for one- and two-electrons systems and for real systems later use kcal/mol. Distances in Å unless otherwise noted.

With exact density  $n_v(\mathbf{r})$  and exact ground-state energy  $E_v[n_v]$ , the (total) energy error (TE) of any self-consistent DFT calculation is:

$$\Delta \widetilde{E}_v = \widetilde{E}_v[\widetilde{n}_v] - E_v[n_v], \tag{5}$$

where  $\tilde{n}_v(\mathbf{r})$  is the self-consistent density of a given approximate functional  $\widetilde{E}_v$ . In DC-DFT this error is split into two well-defined contributions,

$$\Delta \widetilde{E}_v = \Delta \widetilde{E}_F + \Delta \widetilde{E}_D. \tag{6}$$

The functional error (FE) is

$$\Delta \widetilde{E}_{F} = \widetilde{E}_{v}[n_{v}] - E_{v}[n_{v}], \tag{7}$$

i.e., the error the approximate functional  $\widetilde{E}_v$  makes on the exact density  $n_v(\mathbf{r})$ . If the approximate calculation is a KS calculation with an approximate XC functional,  $\widetilde{E}_{\rm XC}[n]$ , its error is a pure density functional of any density  $n(\mathbf{r})$ 

$$\Delta E_{\rm XC}[n] = \widetilde{E}_{\rm XC}[n] - E_{\rm XC}[n], \tag{8}$$

and the FE is just that functional on the exact density:

$$\Delta \widetilde{E}_{\rm F} = \Delta E_{\rm XC}[n_v]. \tag{9}$$

The remaining error is defined as the density-driven error (DDE):

$$\Delta \widetilde{E}_{D} = \widetilde{E}_{v}[\widetilde{n}_{v}] - \widetilde{E}_{v}[n_{v}]. \tag{10}$$

Most DFT errors are dominated by the FE, which we call *normal*, but sometimes DDEs are significant. Such calculations were originally labeled *abnormal*, and could be spotted by a small HOMO-LUMO gap.<sup>2</sup> These were later found to be sufficient but not necessary conditions. In particular, more accurate functionals would often have smaller errors, not dominated by gaps, but still significantly reduced by using better densities. In this work specifically, we refer to Eqs. 7 and 10 as pragmatic errors. By the variational principle, pragmatic-DDEs of total energy are always negative.

Several points are worth noting. First, while all these formulas have been given for the total energy of a specific moiety, in practice, they are applied to the energy differences that are used in chemical and material calculations. A second point is that the HF density has not been mentioned. These are general formulas that in principle can be applied to any system, if the ingredients are available (usually highly accurate energies and densities). We also note that DDEs are only defined using the self-consistent density  $\tilde{n}_v(\mathbf{r})$  of a given approximate  $\tilde{E}_{\rm XC}$ , because the variational principle is hard-wired into their definition. Finally, we mention that this pragmatic-DDE depends both on the system and the approximate functional in use.

For any potential  $v(\mathbf{r})$  and approximate functional, we define the following density functional

$$\widetilde{D}_v[n] = \widetilde{E}_v[n] - \widetilde{E}_v[n_v], \tag{11}$$

which matches the pragmatic-DDE if  $n(\mathbf{r})$  is the self-consistent density of  $\widetilde{E}_v$ , and also correctly vanishes if  $n(\mathbf{r})$  is the exact density  $n_v(\mathbf{r})$ . This formula was defined in Ref. <sup>20</sup> in Eqs. 18 and 19 under the name "density-driven difference", but has been used uncritically as if it yields the DDE of a HF-DFT calculation. For reasons that will become clear, we refer to this as the naive density-driven error interpolator (NDI)  $^{12-16,21}$ .

#### II2. Practicalities

If DC-DFT always required using the exact density, it would not be very useful. In most practical DC-DFT calculations, the (unrestricted) HF density is employed as a pragmatic choice for implementing density correction, since it is generally assumed to be more reliable than the self-consistent density in abnormal situations. 22 In fact, one usually finds that HF densities do little harm in normal calculations, so one can often use them everywhere. 7 Such calculations are dubbed HF-DFT. They predate DC-DFT, but largely because originally DFT was tested on HF densities <sup>23-26</sup>, assuming DDEs were irrelevant. While they significantly improve energetics for abnormal calculations, they have the practical drawback of violating the Hellmann-Feynman theorem, and so need additional terms to calculate forces. 26,27 Moreover, if the UHF calculation is highly spin contaminated, that suggests its density is not accurate, and restricted open-shell HF (ROHF) densities are used instead.<sup>7</sup>

Almost all DC-DFT calculations reported have been for molecular systems. Specific examples include reaction barrier height <sup>25,26</sup>, torsional barrier <sup>28</sup>, halogen and chalcogen bonds <sup>29,30</sup>, anions <sup>31</sup>, most stretched bonds <sup>11,32</sup>, water simulation <sup>33–40</sup>, and many other chemical properties <sup>27,41,42</sup>. A practical criterion to assess abnormality in DC-DFT is to compute the density sensitivity, <sup>43</sup> which is defined as the difference in energy obtained by evaluating the approximate functional on two qualitatively different densities—typically those from HF and the local density approximation (LDA):

$$\widetilde{S} = \left| \widetilde{E}[n^{\text{LDA}}] - \widetilde{E}[n^{\text{HF}}] \right|$$
 (12)

A DFT calculation is considered density-sensitive if  $\widetilde{S}>2$  kcal/mol, suggesting that density-correction may change the energetics. Conversely, if  $\widetilde{S}<2$  kcal/mol, the system is deemed density-insensitive, and the choice of density has minimal impact on the energy. Which reactions are density sensitive depends on the choice of approximate functional. This metric helps identify cases where density correction is likely to be important, and works reasonably well for small molecules, but other criteria have been suggested for other cases  $^{44,45}$ . Of course, it is irrelevant if one has access to the exact functional and density, as then the DDE itself can be calculated directly.

An important aspect of DC-DFT is that the accuracy of the density is measured soley in terms of energy. Because density is a function, one can construct infinitely many different measures of the accuracy of a density. <sup>46</sup> But if errors in densities do not translate into significant errors in energy, they are of little practical importance in DFT calculations. <sup>43</sup> By measuring accuracy in terms of energies, one can automatically see the relevance to DFT applications. Despite its name, applications of DFT mostly involve reports of energies as a function of nuclear coordinates. Thus, an important concept introduced

by DC-DFT is the idea of measuring density errors in terms of the actual energy errors reported in calculations. This is the conceptual cornerstone of the theory, and has also been the key to its practical success.

A crucial part of this paper will be the question: What is the DDE of a HF-DFT calculation? A plausible estimate is simply to apply the NDI to the HF density. Some of us even carelessly used that in Fig. 4 of Ref. <sup>12</sup>, without carefully distinguishing it from a proper DDE. But this is NOT the correct formula for DDE of HF-DFT. To see this, write the HF-DFT energy as

$$\widetilde{E}_v^{\rm HF-DFT} = E_v^{\rm HF} + \widetilde{E}_{\rm XC}[n^{\rm HF}] - E_{\rm X}^{\rm HF}[n^{\rm HF}]. \eqno(13)$$

Insert this in Eq. 2 to find:

$$n^{\mathrm{HF-DFT}}(\mathbf{r}) = n^{\mathrm{HF}}(\mathbf{r}) + \frac{\delta(\widetilde{E}_{\mathrm{XC}}[n_v^{\mathrm{HF}}] - E_{\mathrm{X}}^{\mathrm{HF}}[n_v^{\mathrm{HF}}])}{\delta v(\mathbf{r})}.$$
 (14)

There is a complicated correction to the HF density that is impractical to calculate, and is omitted if using the interpolator. The results of the present work imply that using the NDI on the HF density instead of the correct Eq. 14 yields hopelessly inaccurate estimates, undermining all conclusions based on such calculations.

An important, abstract concept for understanding HF-DFT is to imagine an approximate XC functional which, at self-consistency, yields the exact same energy as HF-DFT for every system. Let us call this HF-DFT-XC and imagine we have an explicit formula for it. Because it yields the HF-DFT density of Eq. 14 *self-consistently*, the definition of pragmatic DDE can be applied, and should yield a good estimate of its ideal-DDE. We call this the self-consistent density of an inconsistent evaluation. In our one-electron examples, we find the self-consistent densities of inconsistent evaluations, and they are very different from the density the functional is evaluated on.

## III. THEORY

## III1. Ideal density-driven errors

Here we (re)-introduce  $^{20,43}$  the concept of the ideal density-driven error (ideal-DDE), which is even better than the pragmatic-DDE of DC-DFT, but more difficult to calculate. For any potential  $v(\mathbf{r})$ , it is a density functional defined as:

$$\Delta E_{\rm D}^*[n] = E_v[n] - E_v[n_v]. \tag{15}$$

Like the pragmatic definition, because it is energy-based, it fits just as well with the aims of DC-DFT. But it has two key advantages relative to the pragmatic definition: (a) it is a measure for any density considered as a trial density for a given system, no matter what its origin, and (b) it does

not use an approximate functional for its evaluation. The pragmatic definition applies *only* to self-consistent densities of KS calculations, and uses the approximate functional in its evaluation. The energetic measure of the size of the pragmatic-DDE depends crucially on the accuracy of the approximate functional for that density. The ideal-DDE does not have this flaw, and is a simple metric for measuring the energetic distance of any approximate density for a given potential.

This concept was introduced in Ref. <sup>43</sup>, but just as an abstraction, and a few of its formal properties were then listed in Ref. <sup>20</sup>. However, it has not previously been calculated. Two exact properties are useful here. First, the ideal-DDE of the total energy is never negative, by the variational principle. This is the mirror image of the negativity of the pragmatic-DDE. The difference in sign is due to the exact functional being used. (We will see below that, for good approximations,  $\Delta E_{\rm D}^*[\tilde{n}_v] \approx -\Delta \widetilde{E}_{\rm D}[\tilde{n}_v]$ ). The ideal-DDE is also convex, i.e., if  $n_{\lambda}({\bf r}) = (1-\lambda)n_0({\bf r}) + \lambda n_1({\bf r})$ , then

$$\Delta E_{\rm D}^*[n_{\lambda}] \le (1 - \lambda) \Delta E_{\rm D}^*[n_0] + \lambda \Delta E_{\rm D}^*[n_1], \quad 0 \le \lambda \le 1.$$
 (16)

Moreover, if  $n_1(\mathbf{r})$  is the exact density, the second term vanishes.

For example, consider every reaction energy in every reference database currently in use in chemistry. For every single one, in principle, if we know the exact XC functional, we can calculate this ideal-DDE for any approximate functional's density. All tests of approximate functionals could include both the error in TE and the ideal-DDE, providing an absolute ranking of the accuracy of each functional's density.

However, it is very difficult to calculate this ideal-DDE for most electronic systems because we don't know the exact functional  $E_{\rm XC}$ . Given an approximate density, one must guess the one-body potential (which typically is not Coulombic) for which this is a ground-state density, and find its ground-state energy. The only real-space case in which such calculations were done is Ref.  $^{47}$ , which is a one-dimensional simulacrum of a four H-atom chain. So, such interacting inversions are impractical.

Here, we report such calculations in two special cases where they are feasible. The first is any one-electron system, where we can easily invert the Schrödinger equation for a trial density, and the second is the two-site Hubbard model with 2 fermions, which is used to mimic two-electron systems and illustrate basic theory in DFT.  $^{47}$ 

How does this ideal-DDE compare to the pragmatic definition of Eq. 10? We show in the illustrations in this paper that often a good approximate functional has a pragmatic-DDE that is close to the negative of the ideal-DDE. (The sign flip is simply because the reference functional has changed from the approximate to the exact.) We give a condition that

Table 1: Sum	mary of symbols	, acronyms,	definitions,	equations,	and equation	numbers	throughout t	his paper.
--------------	-----------------	-------------	--------------	------------	--------------	---------	--------------	------------

symbol	acronym	definition	equation	eq.#
$\Delta E_{\mathrm{D}}^{*}[n]$	ideal-DDE	ideal density-driven error	$E_v[n] - E_v[n_v]$	Eq. 15
$\Delta \widetilde{E}_{ m D}$	pragmatic-DDE	pragmatic density-driven error	$\widetilde{E}_v[\tilde{n}_v] - \widetilde{E}_v[n_v]$	Eq. 10
$\widetilde{D}_v[n]$	NDI	naive DDE interpolator	$\widetilde{E}_v[n] - \widetilde{E}_v[n_v]$	Eq. 11
$\widetilde{\mathcal{E}}_D[n_{proxy}]$	Proxy-DDE	density-driven error with proxy density	$\widetilde{E}_v[\tilde{n}] - \widetilde{E}_v[n_{proxy}]$	Eq. 20
$\Delta E_{ ext{XC}}[n]$	XC energy deviation	exchange-correlation energy deviation	$\widetilde{E}_{\mathrm{XC}}[n] - E_{\mathrm{XC}}[n]$	Eq. 8
$\Delta \widetilde{E}_{ m F}$	FE	functional error	$\widetilde{E}_{\mathrm{XC}}[n_v] - E_{\mathrm{XC}}[n_v]$	Eq. 7
$\Delta \widetilde{E}_v$	TE	total error	$\widetilde{E}_v[\widetilde{n}_v] - E_v[n_v]$	Eq. 5

guarantees this, and most approximations in most calculations seem to meet this condition. When that condition is met, the difference between the FE and the ideal-DDE yields approximately the TE. Table 1 provides a summary of errors in symbols, acronyms, definitions, equations, and equation numbers discussed in this paper.

## III2. Measuring density errors

DDEs (pragmatic or ideal) involve a finite difference of a given functional on two (presumably) very similar densities. These energy differences are typically smaller than the energy errors made by density functional approximations for chemical energy differences. Determining if methods are sufficiently accurate, and have been sufficiently well-converged with respect to a basis set, is highly non-trivial. Many of these issues are discussed in detail in Ref. <sup>12</sup>.

As noted in a previous section, highly accurate methods such as coupled-cluster have been developed to yield accurate energy differences between configurations of atoms. We know of no systematic study that checks the accuracy of the corresponding density (and what would one check it against, anyhow?). Throughout the present work, we assume that the CCSD or CCSD(T) densities for small systems is sufficiently accurate as to introduce negligible error in calculating DDEs.

As a practical implementation of DC-DFT, HF densities are commonly used as proxies for the exact density. Here, we refer to such densities as *practical proxies*, meaning that their computational cost is not typically much higher than, e.g., a hybrid DFT calculation itself. The recent literature has suggested several other densities that are used in place of accurate densities, to test the efficacy of DC-DFT. We call these *proxy benchmark densities*. Clearly, to be useful in DC-DFT at all, these benchmark proxy densities should introduce errors in DDEs that are significantly smaller than the DDEs themselves. Ideally, they should have errors much smaller than the ideal-DDE of HF and self-consistent densities. We shall see that this is an extremely difficult standard to meet in practice (see section V1).

As has already been mentioned, DC-DFT provides just one of infinitely many ways of measuring errors in densities. But because chemical reaction energies are in fact energy differences of different configurations of nuclei, DDEs are typically only reported for such differences. In many such calculations, total energies of the individual moieties are unlikely to be well converged, as differences converge much faster with respect to the basis set. But most other measures of density error that appear in the literature apply only to the density of a given moiety, not the density difference when nuclei are rearranged. Measures that apply only to densities, and not differences of densities, are difficult (if not impossible) to relate directly to the efficacy of DC-DFT. From a different perspective, this is one of the huge benefits of the DC-DFT DDE construction that it can be applied directly to the energy differences that are all important in applications.

#### III3. Functional interpolation

For any given approximate XC functional, we can imagine a one-dimensional family of XC approximations:

$$\widetilde{E}_{\mathrm{XC},a}[n] = (1-a)\,\widetilde{E}_{\mathrm{XC}}[n] + a\,E_{\mathrm{XC}}[n].\tag{17}$$

For  $0 \le a \le 1$ , this interpolates between the approximate  $(a=0,\widetilde{E}_{\rm XC})$  and exact  $(a=1,\ E_{\rm XC})$  functionals. Solving the KS equations with this functional yields an approximate density  $n_a({\bf r})$  parameterized by a. If we extend the construction to any real value of a, this defines a one-dimensional line in density space, and the interpolation is the line segment where a runs from 0 to 1. For sufficiently accurate XC approximations, one would expect the density to vary approximately linearly with a between 0 and 1, but also to always be able to find extreme values of a where non-linearities are noticeable. For simple cases (one-electron), we can find the exact XC functional, but not in practical applications of DC-DFT. Note also that different approximate XC functionals yield distinct families of densities, which coincide only at a=1.

#### IV. RESULTS FOR MODEL SYSTEMS

## IV1. One electron systems

This section reports DC-DFT results for one-electron systems only. This is because the exact functional is easy to calculate in this case, by simply doing a HF calculation, which is self-interaction free. This in turn allows us to perform self-consistent calculations for the functional interpolation (Eq. 17) of any approximate functional, and output its self-consistent density  $n_a(\mathbf{r})$ . Almost all the DDEs reported here are negligible, so DC-DFT has little practical benefit. But the results demonstrate general principles that cannot be deduced from practical calculations.

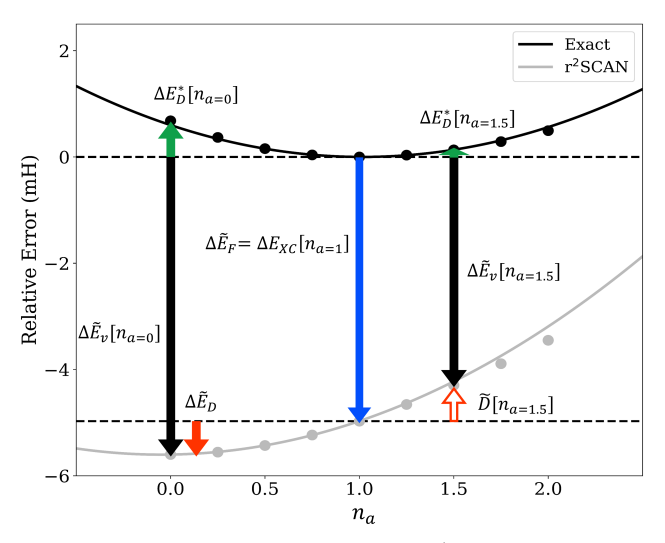


**Figure 1:** Energy error curves of  $\mathrm{H_2}^+$  at equilibrium for r^2SCAN (gray) and exact (black) evaluated on the family of densities  $(n_{a=0})$  minimizing the interpolation functional of Eq. 17. The solid arrows are the total (TE, black, Eq. 5), pragmatic density-driven (DDE, red, Eq. 10), and functional (FE, blue, Eq. 7) errors for r^2SCAN, with ideal-DDE in green. The red hollow arrow is  $\widetilde{D}[n_{a=1.5}]$ , a terrible approximation to (minus) its ideal-DDE (right green arrow, Eq. 15). Any density with 0 < a < 2 is more accurate than r^2SCAN's, and all 1 < a < 2 have smaller TEs (right, black) than the FE of the self-consistent r^2SCAN.

Figure 1 is the most important figure of this paper, and explains a significant fraction of its basic message. These are energy curves for  $\mathrm{H}_2^+$  at equilibrium (geometries of one-electron systems are provided in Table S1), using the  $\mathrm{r}^2\mathrm{SCAN}^{48}$  functional, but are typical of many systems and many approximate functionals (more examples are shown in the Figs. S1-S5). The x-axis is a in Eq. 17 and the density at each value is the self-consistent density  $(n_a(\mathbf{r}))$  with that a. The solid black curve is the exact energy for each density, with the zero chosen at the exact energy, and the solid gray curve is the  $\mathrm{r}^2\mathrm{SCAN}$  energy. The black and red arrows on the left (a=0) denote TE and

DDE, respectively. While the blue arrow in the middle (a=1) denotes the FE of r<sup>2</sup>SCAN.

The first point to note is that the value of the black curve is the ideal-DDE for each of the densities. To the extent that these densities are linear in a, this curve must be convex and typically is close to a simple parabola. Next we note that  $\Delta E_{\rm D}^*[\tilde{n}] \approx -\Delta \widetilde{E}_{\rm D}$ . We will show numerous systems and functionals where this is true to within about 20 %. Figure 2 shows the density errors with respect to exact density, as a function of a, which are clearly (almost) proportional to 1-a. Assuming linearity, this implies that the black-(exact)-curve in Fig. 1 is convex, as in Eq. 16. Moreover, it must always be parabolic on a small enough scale around a=1. The closer the self-consistent density is to the exact density, the closer the ideal-DDE curve will be to a parabola.

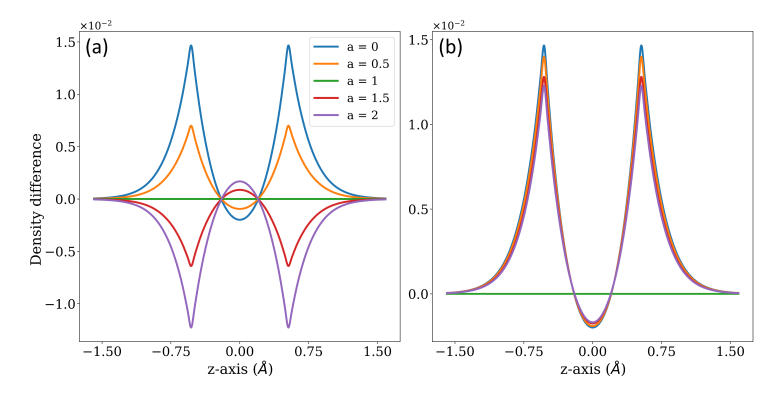


**Figure 2:** (a) Density errors of  $r^2SCAN$  from Eq. 17 and (b) density errors  $\div(1-a)$  of  $H_2^+$  at equilibrium along z-axis.

Next we explain one of the most important aspects of this work. All densities with a between 0 and (about) 2 are more accurate than the self-consistent density (a=0). i.e., they have smaller ideal-DDEs. In Table 2, we list three fomrulas for DDEs as a function of a (more examples are shown in Tables S2-S6). The first is the ideal. The second is the pragmatic, using the appropriate a-dependent functional for each value of a, as given by Eq. 10. It tracks the ideal very well, as expected. But the third uses the original functional (a=0) to estimate the DDE at the intermediate points via Eq. 11, i.e., the NDI. While it is indeed correct at the two points (a=0), and 1), it becomes more and more relatively inaccurate as a approaches 1, and nonsensical for a>1, as its estimate of the pragmatic-DDE has the wrong sign!

Consider the functional with a=0.75 and its associated density. Its ideal-DDE is much smaller than that of the self-consistent density, and the r²SCAN functional evaluated on this density,  $n_{a=0.75}(\mathbf{r})$ , almost exactly reproduces the FE, precisely as the naive understanding of DC-DFT expects. However, a more interesting comparison is with a=1.5. This is still a much better density than the self-consistent density. But now the TE r²SCAN makes on this density,  $n_{a=1.5}(\mathbf{r})$ , is even

**Table 2:** Ideal- and pragmatic DDEs, and NDI (in mH) of  $\rm r^2SCAN$  at densities depending on the mixing parameter a in  $\rm H_2^+$  at equilibrium. In the pragmatic row, the XC functional changes according to Eq. 17 but, in the naive row, only  $\rm r^2SCAN$  is used in Eq. 11.

(mH)	value of $a$									
$_{\mathrm{type}}$	0.00	0.25	0.50	0.75	1.00	1.25	1.50	1.75	2.00	
ideal	0.68	0.37	0.16	0.04	0.00	0.04	0.13	0.29	0.50	
prag.	-0.63	-0.35	-0.15	-0.04	0.00	-0.04	-0.14	-0.31	-0.53	
naive	-0.63	-0.58	-0.46	-0.26	0.00	0.32	0.68	1.08	1.52	

smaller than the FE ( $|\Delta \widetilde{E}_v[n_{a=1.5}]| < |\Delta E_{\rm XC}[n_{a=1}]|$ ). This is simply because a>1 and the difference between the two curves, that is,  $\Delta E_{\rm XC}[n_a]$  continues to shrink.

However, suppose we imagined that the NDI (Eq. 11) was an accurate measure of DDE. Its estimate of the DDE of  $n_{a=1.5}(\mathbf{r})$  has the wrong sign, and is a large overestimate (red hollow arrow upwards in Fig. 1), compared with the tiny green arrow at a=1.5. For this density, it appears that the DDE is larger than that of the self-consistent density, and that its removal leads to a smaller energy error, a highly fortuitous cancellation of errors with FE that only gets better as a increases. However, as we can see, the ideal-DDE is much smaller, there is no significant cancellation of errors, and it is perfectly natural to have an energy error smaller than the FE. In fact, it is unavoidable once a is between 1 and 2.

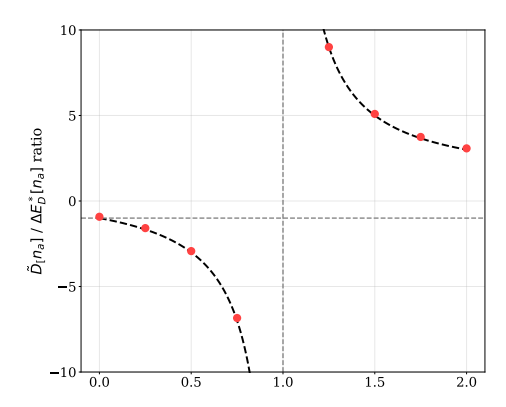


**Figure 3:** Naive density-driven error (DDE) interpolator (NDI) versus ideal-DDE ratio for  $r^2SCAN$  in  $H_2^+$  at equilibrium. Red dots are the values of a for each density, and black dashed line is (1+a)/(a-1) curve. The gray horizontal lines denote y=-1. The x-axis is the same as in Fig. 1.

In Fig. 3, we plot the ratio of the NDI to the ideal-DDE as a function of a, showing the divergence. Assuming linearity in the density and parabolic functionals, one finds this curve has shape (1+a)/(a-1), plotted with dashes in the figure. (The ideal-DDE is proportional to  $(a-1)^2$ , and the NDI is proportional to  $(a^2-1)$ .) Thus, for a=1.5, the overestimate is a factor of 5. The NDI always overestimates, and the more accurate the density is, the greater the relative inaccuracy!

**Table 3:** Ideal- and pragmatic density-driven error (DDE), functional error (FE), and total error (TE) in mH for  $\mathrm{H}_2^+$  at equilibrium. Molecular energy followed by binding energy.

(mH)	type	${ m r^2SCAN50}$	$\text{LC-}\omega\text{PBE}$	SVWN	${ m r^2SCAN}$	B3LYP	PBE	BLYP			
total energy											
DDE	ideal	0.16	0.62	0.66	0.68	0.91	1.25	1.62			
DDE	prag.	-0.15	-0.57	-0.63	-0.63	-0.84	-1.14	-1.47			
FE		-2.49	-10.68	19.48	-4.97	-6.66	-5.52	-3.06			
$^{\mathrm{TE}}$		-2.64	-11.25	18.85	-5.60	-7.50	-6.66	-4.53			
			bind	ing energy	,						
DDE	ideal	0.11	0.32	-0.37	0.49	0.51	0.60	0.88			
DDE	prag.	-0.11	-0.29	0.36	-0.45	-0.47	-0.56	-0.81			
FE		-2.49	-4.69	-2.84	-4.97	-4.59	-6.11	-5.81			
TE		-2.60	-4.98	-2.48	-5.43	-5.06	-6.67	-6.62			

To show that none of these features are specific to this functional, in Table 3, we listed ideal- and pragmatic-DDEs of several popular approximate functionals and two proxy functionals in Ref.  $^{13-16}$  (r²SCAN , B3LYP  $^{49}$ , PBE  $^{50}$ , BLYP  $^{51,52}$ , SVWN  $^{53,54}$ , r²SCAN50  $^{55}$ , and LC- $\omega$ PBE  $^{56}$ ) on the H $_2^+$ , ordered by their ideal-DDEs (CAM-B3LYP  $^{57}$  and PBE0  $^{58}$  on SI). With this measure, we can also say they are ordered in terms of the accuracy of their densities. We see that in every case, the size of the ideal-DDE is about 10 % larger than the corresponding absolute pragmatic-DDE value. Moreover, ordering with respect to the pragmatic-DDE is almost identical to that of the ideal-DDE (in Fig. S1 we also illustrate each of these functionals with curves analogous to Fig. 1, but keep in mind that the densities being scanned through as a function of a differ in every case).

Table 4: Density-driven errors (DDE) in mH of  ${\rm H_2}^+$  at the equilibrium using naive density-driven error estimate of Eq. 11. Only diagonals (shaded) are the correct pragmatic-DDEs. The range refers to the range of naive DDE interpolator (NDI) predicted by the functionals for a given density. The aug-cc-pV5Z basis set was used.

	(mH)	r <sup>2</sup> SCAN50	LC-ωPBE	SVWN	density r <sup>2</sup> SCAN	B3LYP	PBE	BLYP
	$\rm r^2SCAN50$	-0.15	0.03	0.17	0.03	0.17	0.39	0.62
-	$LC-\omega PBE$	-0.40	-0.57	-0.29	-0.49	-0.50	-0.45	-0.30
one	SVWN	-0.32	-0.35	-0.63	-0.33	-0.37	-0.24	-0.09
Ġ.	$r^2SCAN$	-0.46	-0.55	-0.32	-0.63	-0.57	-0.47	-0.38
functional	B3LYP	-0.53	-0.77	-0.58	-0.78	-0.84	-0.80	-0.75
444	PBE	-0.63	-1.02	-0.75	-0.99	-1.09	-1.14	-1.09
	BLYP	-0.74	-1.20	-0.93	-1.22	-1.37	-1.42	-1.47
	range	0.59	1.23	1.10	1.25	1.54	1.81	2.09
	ideal-DDE	0.16	0.62	0.66	0.68	0.91	1.25	1.62

To show that the poor performance of the NDI is not somehow an artifact of our special family of densities, Table 4 presents a matrix of different approximate functionals applied to each other's self-consistent densities. The diagonals are the correct pragmatic-DDEs, and all others are (incorrect) estimates using Eq. 11. From their variation, it is clear that none are reliable, and  $\rm r^2SCAN50$  even producing incorrect signs, just as we found for a>1 in our model example. For this system, we conclude that the pragmatic-DDE is a good estimate of the ideal-DDE, but the NDI is highly inaccurate anywhere except at the self-consistent densities.

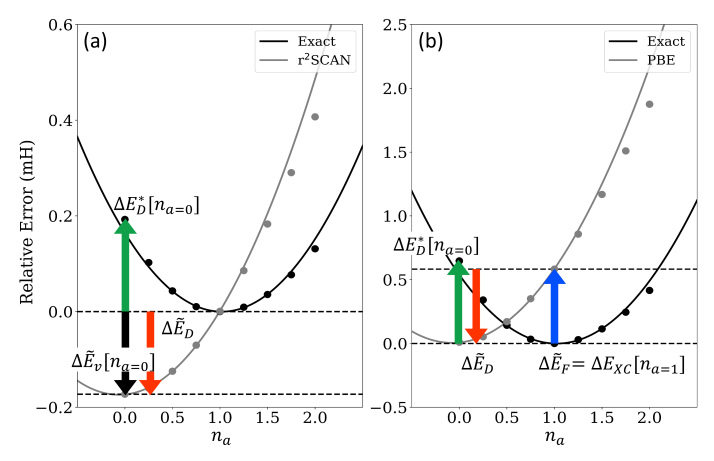


**Figure 4:** Two atypical cases: Exact (black) and DFT (gray, (a)  $r^2SCAN$  and (b) PBE) energy functionals for the hydrogen atom, evaluated on the family of densities minimizing the interpolation functional of Eq. 17. Points are evaluations, and curves are parabolas that fit to the curvature at the minimum. The green (red) arrow shows the ideal (pragmatic) density-driven error, the blue shows the functional error, and the black denotes the total error.

Why did we not illustrate our points with the simplest of all one-electron systems, the H-atom? We did not choose this because the behavior of two of the most popular functionals (PBE and r<sup>2</sup>SCAN) is untypical in this case. However, both provide nice illustrations of DC-DFT principles. r<sup>2</sup>SCAN was chosen with the exact condition (norm) that, on the exact H-atom density, it yields the exact H atom energy of -1/2 (in Hartree). <sup>59</sup> Despite this, it makes a small error for the H atom, as its self-consistent density is not a simple exponential (see Fig. 4(a)), and it is about -0.173 mH lower in energy. True to its construction, that error vanishes at the exact density, so its error is entirely density-driven. The ideal-DDE agrees with the pragmatic-DDE to within about 10%. Thus, evaluation of r<sup>2</sup>SCAN on the exact density reduces the error to essentially zero, i.e., the posterchild of DC-DFT calculations, but hardly a typical case. On the other hand, the PBE functional shows a very different atypical behavior (see Fig. 4(b)). It was long ago shown that, self-consistently, PBE is essentially perfect for the H atom energy. So this is an example of FE and DDE canceling exactly. Thus, here, swapping in the exact density only worsens the energy, and this is not a calculation that is improved. What DC-DFT does do is tell us that these perfect results is in fact an accidental cancellation of the two errors.

How does this ideal-DDE connect to (pragmatic) DC-DFT? The most appealing definitions are Eq. 7 for the FE, and Eq. 15 for the ideal-DDE. But these two do not in general combine to yield the TE. The answer is simple. We continue to use the usual (pragmatic) DDE in DC-DFT (Eq. 10), as it is the only one we can calculate without recourse to the exact functional on approximate densities, which is rarely available. However, we consider it typically a good approximation to the ideal,

and assume that is the case for most functionals in common use (i.e., those yielding useful accuracy for the problem at hand). Thus, for a given potential, different approximations will produce different self-consistent densities, with different DDEs. But if the curvature of the approximation is good, its DDE is an excellent estimate of its ideal-DDE, and it can be directly compared, as in Table 3.

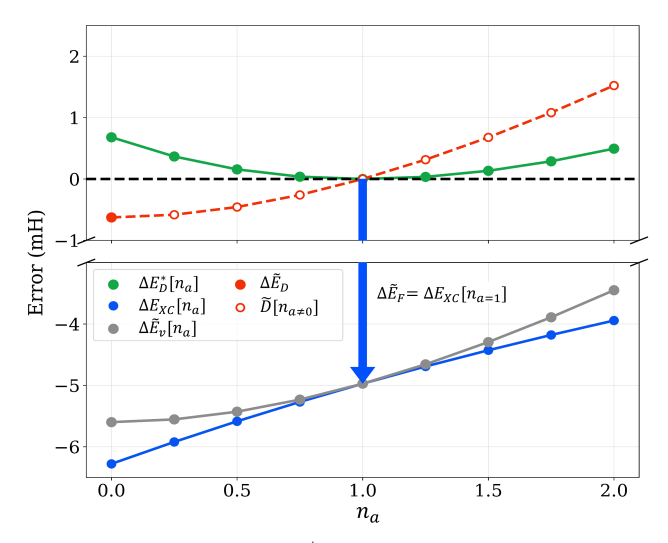


Figure 5: Error curves of  $\mathrm{H_2}^+$  at equilibrium for r²SCAN. ideal-DDE ( $\Delta E_{\mathrm{D}}^*[n_a]$ , green dots, Eq. 15), pragmatic-DDE ( $\Delta \widetilde{E}_{\mathrm{D}}$ , filled red dot, Eq. 10), NDI ( $\widetilde{D}[n_{a\neq 0}]$ , hollow red dots, Eq. 11), FE ( $\Delta E_{\mathrm{XC}}[n_{a=1}]$ , blue arrow, Eq. 7), XC energy deviation ( $\Delta E_{\mathrm{XC}}[n_a]$ , blue dots, Eq. 8), and TE ( $\Delta \widetilde{E}_v[n_a]$ , gray dots, Eq. 5). Even at a=2, where the ideal-DDE matches that of the self-consistent density, the total error is reduced because the reduction in  $\Delta E_{\mathrm{XC}}$  is greater than the increase in  $\Delta E_{\mathrm{D}}^*$ .

Alternatively, there is a formulation of DC-DFT that uses the ideal-DDE, but combines it with the (equally impractical) functional error evaluated on the approximate density:

$$\Delta \widetilde{E}_v \approx \Delta E_{\rm XC}[\tilde{n}_v] + \Delta E_{\rm D}^*[\tilde{n}_v]$$
 (18)

This formulation also yields the TE but from a slightly shifted perspective. Figure 5 shows the information in Fig. 1 more dynamically. Using a density closer to the exact density than the self-consistent one reduces TE (gray dots) by both lowering the ideal-DDE (green dots) and narrowing the gap between approximate and exact functionals at that density point ( $\Delta E_{\rm XC}$ , blue dots). This explanation describes how, from a total energy perspective, certain DC-DFT calculations can achieve smaller errors than FE. The values are in Table 5. But this description is true when the approximate functional curve lies below the exact. If the curves have similar minima, or even if the approximate curve is located above the exact curve (situation like SVWN in Fig. S1), then as the density becomes more accurate (closer to a=1), the TE increases.

Our final discussion of energy curves for our one-electron cases fills in some details beyond Fig. 1. Figure 6 shows several

**Table 5:** Ideal density-driven error (DDE), exchange-correlation energy deviation ( $\Delta E_{\rm XC}[n_a]$ ), and total error (TE, in mH) of r<sup>2</sup>SCAN at densities depending on the mixing parameter a in  ${\rm H_2}^+$  at equilibrium.

(mH)	value of $a$								
type	0.00	0.25	0.50	0.75	1.00	1.25	1.50	1.75	2.00
ideal-DDE	0.68	0.37	0.16	0.04	0.00	0.04	0.13	0.29	0.50
$\Delta E_{\rm XC}[n_a]$	-6.28	-5.92	-5.59	-5.27	-4.97	-4.69	-4.43	-4.18	-3.94
$^{\mathrm{TE}}$	-5.60	-5.56	-5.43	-5.23	-4.97	-4.69	-4.30	-3.89	-3.45

different parabolas, and a purple line connecting their minima. The gray and the black are the original approximate and exact functionals, respectively. We consider evaluating the original approximation on the a=1.5 density. Its functional is plotted in green. This is a better density than the self-consistent density, and yields a smaller error than the FE.

The purple line is the minimizing energy of the family of functionals given in Eq. 19 and parameterized by a. We draw a horizontal line to find where its energy matches that of the inconsistent evaluation, which happens at a=0.22. The blue parabola is the energy of that functional. A careful analysis, assuming curves are parabolic in a and densities are linear, yields the following equation for b:

$$b \simeq (a^2 - b^2) \frac{\Delta \widetilde{E}_{\rm D}}{\Delta E_{\rm XC}[\tilde{n}]}$$
 (19)

Note that b is typically small in this scenario (Table 6), because of the ratio of the energies. Also plotted in the figure is the result of our formula, both with and without the  $b^2$  term. We assume that the above equation holds provided the minima of the curves lie approximately on a straight line.

The importance of this result is that, in fact, with the approximations we have made, this density at b is the self-consistent density of the functional that reproduces the inconsistent result (ignoring any potential dependence of b in Eq. 19, which is likely to be small). So this explicitly shows (a) that the density of the inconsistent calculation is far from the HF density, nullifying any rationale for using the NDI, (b) that it seems likely to be quite close to the original self-consistent density, and (c) it is more accurate than the self-consistent density (its DDE is smaller). This functional has both better energies and better densities than the original, i.e., both its FE and DDE are smaller than the original.

**Table 6:** The value of b according to a in Eq. 19 with  $r^2$ SCAN functional in the  $H_2^+$  equilibrium.

	value of $a$										
type	0.00	0.25	0.50	0.75	1.00	1.25	1.50	1.75	2.00		
b	0.0	0.01	0.02	0.06	0.10	0.15	0.22	0.30	0.38		

Finally, we close by studying stretched  $H_2^+$ , the paradigm of

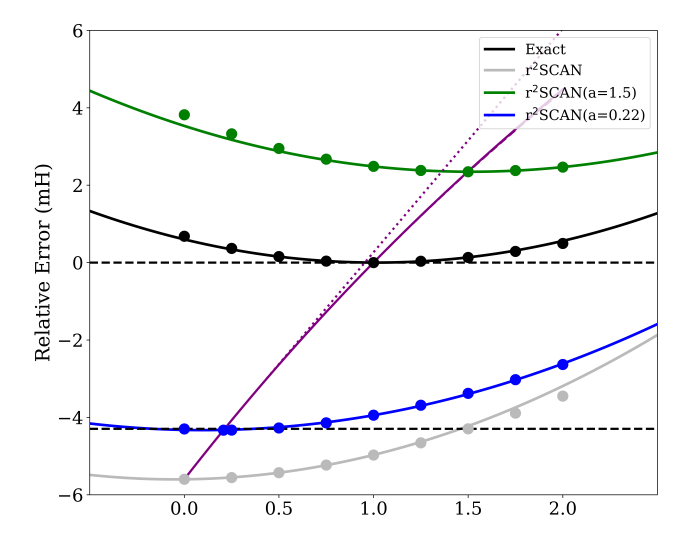


Figure 6: Energy error curve at a=1.5 in Eq. 17 (green) and energy error curve at a=1.5 estimated according to Eq. 19 (b = 0.22, blue). The purple solid line is the spline of the self-consistent energy error of the Eq. 17 functional according to the b value estimated through Eq. 19. The purple dotted line is the linear spline of the self-consistent energy error of the Eq. 17 functional based on the estimated b value obtained by removing the quadratic term of b from Eq. 19.

**Table 7:** Ideal- and pragmatic-DDE, FE, and TE in mH for (top)  $H_2^+$  at 5Å and (middle) H atom. The bottom is the contribution to the binding energy.

(mH)	type	$\rm r^2SCAN50$	$\text{LC-}\omega\text{PBE}$	SVWN	${ m r^2SCAN}$	B3LYP	PBE	BLYP				
	$\mathrm{H_2^+}$ at 5Å total energy											
DDE	ideal	4.60	3.46	5.11	5.56	2.42	1.16	2.08				
DDE	prag.	-4.66	-3.52	-5.18	-5.41	0.35	-1.18	-1.97				
$_{\mathrm{FE}}$		-63.39	-63.52	-74.25	-75.18	-49.23	-31.69	-28.35				
$^{\mathrm{TE}}$		-68.05	-67.04	-79.43	-80.60	-48.88	-32.87	-30.32				
	H atom total energy											
DDE	ideal	0.04	0.30	1.02	0.19	0.40	0.65	0.74				
DDE	prag.	-0.04	-0.28	-0.99	-0.17	-0.37	-0.57	-0.66				
FE		0.00	-5.99	22.32	0.00	-2.07	0.58	2.74				
$^{\mathrm{TE}}$		-0.04	-6.27	21.33	-0.17	-2.44	0.01	2.09				
			$\mathrm{H_2}^+$ at $5\text{\AA}$	binding	energy							
DDE	ideal	4.55	3.16	4.09	5.37	2.02	0.52	1.34				
DDE	prag.	-4.62	-3.23	-4.19	-5.24	0.72	-0.60	-1.31				
$_{\mathrm{FE}}$		-63.39	-57.53	-96.57	-75.18	-47.16	-32.28	-31.09				
$^{\mathrm{TE}}$		-68.01	-60.77	-100.76	-80.42	-46.44	-32.88	-32.41				

self-interaction error  $^{10}$ . We take the bond length to be 5 Å (Table 7), almost five times of equilibrium bond length. At this distance, any approximate functional with a self-interaction error makes a large error in the energy, because it is inaccurate for the 1/2-electron densities localized on each proton. As the bond length is stretched to infinity, the energy does not approach that of a single H atom, as it should.

But this is *not* density-driven. This is plain to see in Table 7. Whether looking at the molecular energy or the contribution to the binding energy, the DDE is a small fraction of the FE. The densities are reasonably accurate, and the error is functional-driven. Thus, while DC-DFT is a useful tool for

studying systems with strong self-interaction errors, not all such errors are density-driven. This result is associated with the fact that DC-DFT, as described earlier in Fig. 5, causes error reduction not only through ideal-DDE but also through a decrease in  $\Delta E_{\rm XC}$ . Analogously, DC-DFT can be a useful tool for many other kinds of density errors, not just those caused by self-interaction. This distinction sometimes seems lost in the literature.

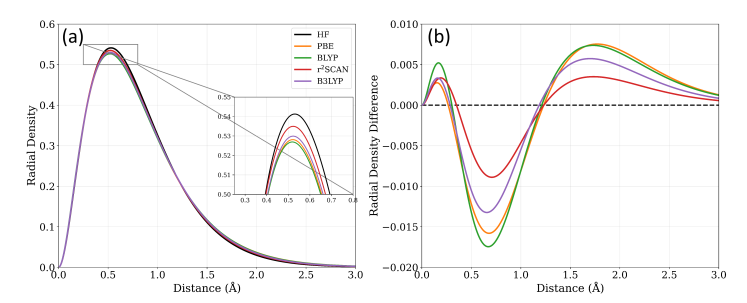
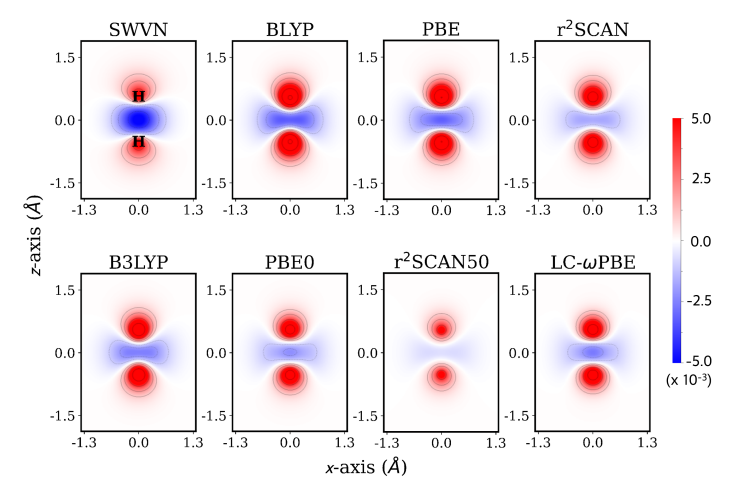


Figure 7: Radial densities (a) and radial density difference (b) of H atom for several functionals.

We close by discussing the relation between plots of density errors and DDEs. In Fig. 7, we show several densities and their errors for the H atom. The panel (a) shows how very close all of them are, and essentially indistinguishable by eye, except when zoomed in. In (b), we plot the errors in the densities, and looking at the minima in that figure, we might decide BLYP is least accurate, followed by PBE, B3LYP, and then  $\rm r^2SCAN$ . Consultation of Table 4 then shows that your intuition is good in this case, and DDEs (ideal or pragmatic) have the same ordering.



**Figure 8:** Contour map of density error  $(n(\mathbf{r}) - n^{\text{HF}}(\mathbf{r}))$  of  $H_2^+$  at equilibrium for several functionals in xy-plane. Unit for density is  $e/\mathring{A}^3$ .

But Fig. 8 shows the density errors for several functionals for  $\mathrm{H}_2^+$ . By visual inspection, try ordering these 8 plots in order of their accuracy. Then compare your relative ordering with the results in Table 4. Chances are high you did not get them right. We have found no simple way to relate density

error plots (or other metrics of density error) to those of DDE. We also point out that it is actually the difference between DDEs that goes into DDEs for reaction differences, such as the binding energy of  $H_2^+$ . It is entirely unclear how to apply any metric of density error to the error in the difference of two densities with different external potentials.

## IV2. Two-electron systems

To further illustrate the crucial distinctions between ideal- and pragmatic- DDE, we use the two-site Hubbard dimer model. The Hubbard dimer is a simplified model of a heteronuclear diatomic molecule, where electrons can hop between two sites and interact only when they doubly-occupy a site. The sites are subject to a potential difference  $\Delta v$  that establishes a site-occupation difference  $n_2-n_1$ . For fixed hopping parameter and interaction strength t and t, the exact two-electron ground-state energy and density can be produced directly as a function of the potential. The associated KS quantities and inversion can be computed exactly, and all functionals can be plotted as functions of the density t

The density of the dimer is a number, with more accurate densities simply being close to that number. However, this is enough to define two qualitatively distinct types of errors for the density, and thus the logic of DC-DFT can be applied directly. The standard density functional approximations typically used in practice are generally not available for the dimer, but we demonstrate DC-DFT principles using unrestricted Hartree-Fock (UHF) and second-order density-functional perturbation theory (GL2)<sup>60</sup>.

For the dimer it is simple to evaluate functionals using a density other than its corresponding self-consistent density. In fact, it is also possible to evaluate the corresponding self-consistent density associated to an inconsistent evaluation of density functional. For example, the GL2 total energy evaluated with the Hartree-Fock density  $E^{\rm GL2}(n_1^{\rm HF}(\Delta v))$ . The derivative with respect to  $\Delta v$  yields the associated density of all functionals, including the self-consistent density of the inconsistent evaluation, as discussed in Sec. II2, which is plotted in green in Fig. 9.

In the strongly-correlated regime ( $\Delta v < U$ ), the UHF density is closer to the exact, when compared to the GL2 density. However, UHF is a poorer approximation of the energy, and thus provides a range of parameters where DC-DFT can be demonstrated. The density associated to the inconsistent evaluation of the GL2 functional with the UHF density, the green curve of Fig. 9, provides a slight improvement over the GL2 self-consistent density.

Figure 10 is a generalization of Fig. 1, and the exact groundstate and HF density functionals are evaluated with a self-

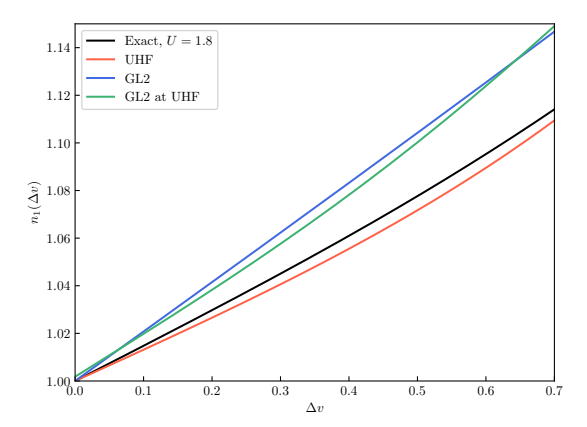


**Figure 9:** Exact (black), unrestricted Hartree-Fock (red), second-order Görling-Levy perturbation theory (blue), and inconsistent evaluation of GL2 density functional with UHF density (green).

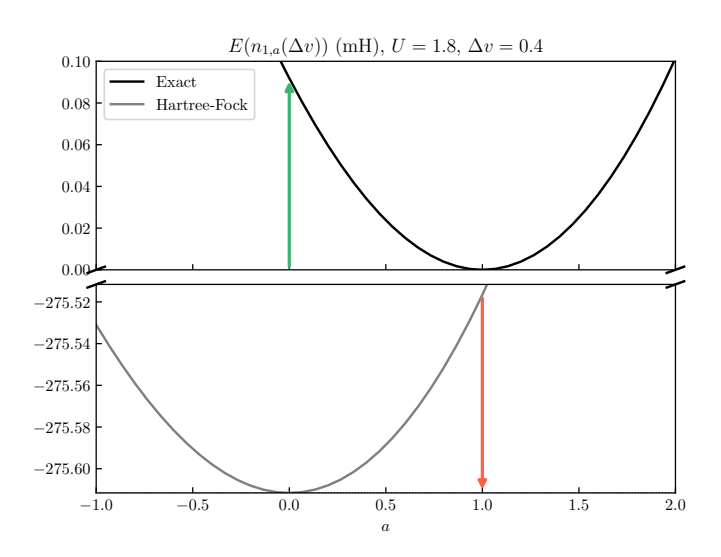


**Figure 10:** Exact (black) and UHF (gray) density functionals evaluated at density  $n_{1,a}(\Delta v)$ , which interpolates between Hartree-Fock (a=0) and exact (a=1). The green and red are ideal and pragmatic density-driven errors respectively. Both curves are shifted by their respective "atomic-limit" values, where hopping  $t \to 0$ .

consistent density  $n_{1,a}(\Delta v)$ , where  $0 \leq a \leq 1$  interpolates between pure HF exchange (a=0) and exact total XC (a=1). In this interacting case, the pragmatic- and ideal- DDEs are roughly equal and opposite. This trend continues over the range of plotted  $\Delta v$  values. From Fig. 11, at  $\Delta v = 0.4$  the pragmatic-DDE is comparable in magnitude to the ideal. As  $\Delta v$  increases, the dimer becomes weakly correlated, and for all plotted parameters, minus the pragmatic-DDE remains within  $\pm 10~\%$ .

Figure 12 is analogous to Fig. 6. We observe that the self-consistent GL2 density is further from the exact ( $a\approx 0.7$ ), and the total error in the energy is roughly -70 mH. The Hartree-Fock provides a poor approximation to the energy,

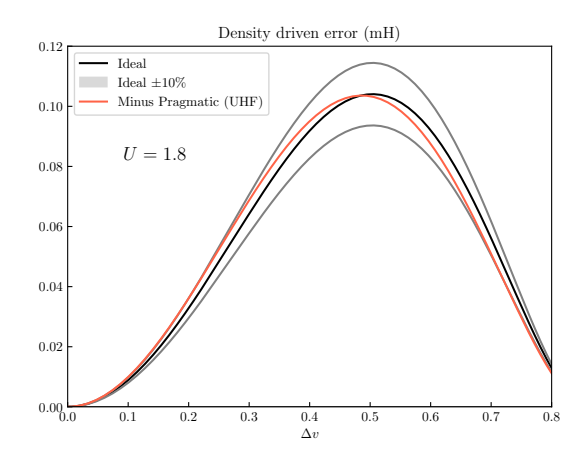


Figure 11: Ideal (black) and minus the pragmatic (red) density-driven errors plotted for a range of external potentials. The shaded regions are  $\pm 10$  % the ideal-DDE. Minus the pragmatic-DDE is within the shaded regions for many values of strongly-correlated  $\Delta v < U$ .

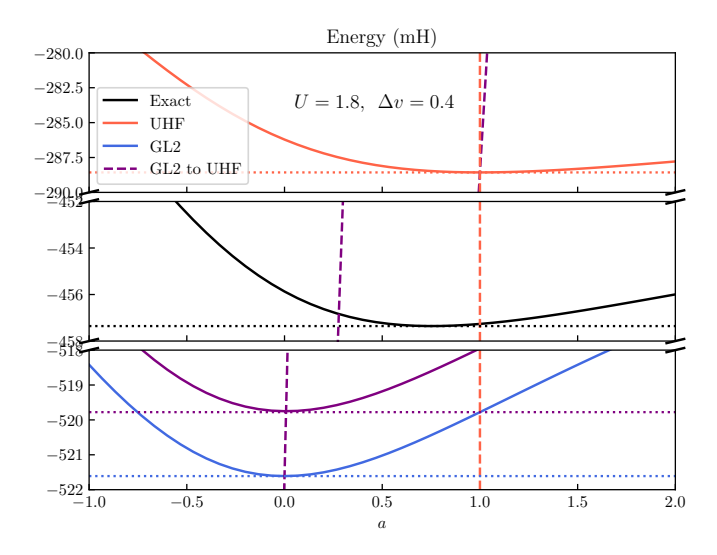


Figure 12: Exact (black), unrestricted Hartree-Fock (red), and second-order density-functional perturbation theory (blue) energies, density-corrected (purple). Here self-consistent densities are denoted with dashed vertical lines. The density-corrected energy (dotted purple) is the improved prediction of the energy by substituting the Hartree-Fock density into the GL2 functional.

but the self-consistent UHF density is closer to the exact. Thus, the density correction provided by the UHF density reduces the total error slightly by reducing the DDE. We plot exact and approximate density functionals evaluated with  $n_{1,a}(\Delta v)$ , which interpolates between GL2 (a=0) and HF (a=1). The dashed purple line connects the GL2 and UHF minima, unlike Fig. 6, and the purple dotted line denotes the density-corrected energy. The dashed and dotted purple lines intersect at  $a\approx 0.08$ , which is approximately the minimum of the true density-corrected density-functional corresponding to the inconsistent GL2 evaluation.

## IV3. Summary of model systems

This survey has produced several key concepts in DC-DFT. First, the ideal-DDE is well-defined for every system and depends only on the approximate density, not on an approximate energy functional. Second, the pragmatic-DDE uses the approximate functional to estimate the ideal, typically producing about a 10 % underestimate (and the opposite sign). We found no cases where it was not a good estimate. Third, the use of any density other than the self-consistent density in the NDI almost always fails to give a good estimate of the DDE (ideal or pragmatic).

## V. Practicalities

The previous section was written to demonstrate basic principles of DDEs. But it was confined to either one-electron systems or model two-electron systems. Now we study the realistic cases that have caused controversy in the literature, using the insight garnered from the previous sections.

Why are there questions about how DC-DFT performs its magic? In practice, the HF density often serves as a practical tool for density-correction. Many studies in the literature, using various obvious measures of density errors, suggest that HF densities are less accurate than self-consistent DFT densities. <sup>14,15,61</sup> As mentioned above, and studied below, the difficulty lies in relating those measures to DDEs, especially for chemical energy differences. We have found no simple relationship between such measures and DDEs.

A second issue is how to measure the DDE of an HF-DFT calculation (i.e., an approximate density functional evaluated on the HF density). An essential problem is that we do not know the exact density of such a calculation. Its density is neither the HF density nor the self-consistent density of the approximate functional. It is given by Eq. 13, but we have no practical means to calculate this. The results of the model section yield a better density than the self-consistent one in that specific case, but that method only works there. Then, even if we had this density, we cannot calculate the ideal-DDE without the exact functional, nor can we calculate the pragmatic-DDE without having the pure density functional for which this density is a self-consistent minimum. As we shall discuss, folks have resorted to the NDI, which we have seen bears no relation to true DDEs.

#### V1. Proxy benchmark densities, and their pitfalls

For many systems, it can be extremely challenging to evaluate even the pragmatic-DDE. First, one needs a reliable calculational method that produces highly accurate densities. Then one must perform a Kohn-Sham inversion, i.e., find the KS potential whose ground-state density is the accurate density. This problem has a long and difficult history. <sup>12,28,62–70</sup> Finally, armed with the KS orbitals, one can calculate the approximate functional's energy on the exact density. As this is often not practical for systems of chemical interest, ways have been found to bypass these steps.

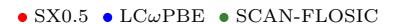
Recent literature has made use of "proxy densities" as standins for the exact density when evaluating DDEs for molecules. For example, Kaplan and others  $^{13}$  present an analysis of DDE and FE for barrier heights, evaluated against three such proxies: SX-0.5, SCAN-FLOSIC, and LC- $\omega$ PBE. The authors estimate DDE using a proxy in place of the exact density  $n_v(\mathbf{r})$ , see Eq. (10):

$$\widetilde{\mathcal{E}}_D[n_{proxy}] = \widetilde{E}_v[\tilde{n}] - \widetilde{E}_v[n_{proxy}].$$
 (20)

If the proxy were the exact density, this becomes the pragmatic-DDE. Each of these proxy methods is an approximate KS-DFT method, and so yields both a density and its corresponding orbitals, thereby making evaluation of  $\widetilde{E}[n_{proxy}]$  simple. But, as discussed earlier, DDEs are typically much smaller than FEs, and one needs to be able to rank self-consistent densities of different functionals. Thus a proxy method needs to be precise enough to distinguish small differences among already small numbers.

In the case that  $n_{proxy}(\mathbf{r})$  is extremely close to the exact density,  $\tilde{\mathcal{E}}_D$  is a good estimate of the pragmatic-DDE. But in the absence of more accurate reference densities, it is impossible to determine the efficacy of a proxy (i.e., quantify how close the proxy is to the exact density). However, if multiple different proxies are suggested, then some tests of internal consistency can be performed. First, when evaluating the DDEs of a set of functionals using the proxies, the ranking of those functionals (i.e., which has the lowest DDE) should be consistent among all the proxies used. Second, for the proxies to be useful, the spread among their estimates of the DDE should be small relative to the DDE itself. If their spread is a significant fraction of the DDE, this would render the proxies dubious as useful estimators.

Here we analyze the results reported in Ref. <sup>13</sup> for the three proxies suggested there, for the DDEs of the BH76 set of barrier heights. We find that in over a third of cases, the proxies disagree on which functional has the lowest DDE (see Table S7). Kaplan et al. <sup>13</sup> point to the consistency of the DDE averaged over the reactions of the three proxies, but this ignores their deviations for each reaction. We stress the importance of examining the proxies on a case-by-case basis, revealing significant inconsistencies which can be obscured by averaging. Figure 13 shows the variations in DDE for their three different benchmark proxy densities and two different functionals, PBE and SCAN across the systems of BH76. The figure should already be alarming, showing some extreme



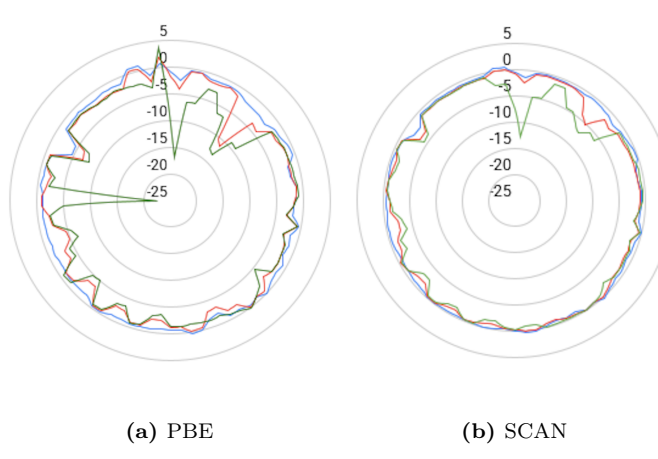


Figure 13: Reaction-by-reaction breakdown BH76. DDEs for PBE and SCAN functionals using the three proxies (in kcal/mol) are plotted on the radial coordinate. The angular coordinate corresponds to the reaction index. In some (density-sensitive) cases, the proxies disagree by more than 20 kcal/mol. The spread of DDEs across the proxies is sensitive to both the functional used, and the system in question.

variations, especially for SCAN-FLOSIC.

For simplicity, we choose the average of the three DDEs (evaluated on the three densities) as the best estimate of the exact DDE, and the spread (max minus min) as an estimate of its uncertainty (reporting the results for all 76 reactions in the Table S7). Table 8 lists results averaged over BH76 of DDE using each of the three proxies and the spread. In fact, the spreads are significant on the scale of the DDEs themselves. Furthermore, examining the DDEs of the RKT10 transition state barrier (Table 9), for which a high-accuracy reference is available, we see that the proxies are essentially useless, as their spread is larger than the known DDE itself. Finally, analyzing the density sensitivities of the BH76 systems (calculated in Ref. 8) shows that the reactions with the widest range of DDEs across the proxies are generally highly density-sensitive. We present some of the worst cases in Table 10; and it is precisely in these cases that the application of the HF density tends to cure the errors.8

**Table 8:** Uncertainties due to proxy benchmarks on BH76 dataset, calculated from data presented in the SI of Ref. <sup>13</sup>: Mean and mean range of DDE calculated with three different proxy densities, averaged over BH76. The deviation among the proxies is comparable to the DDEs themselves.

functional	avg. DDE (kcal/mol)	avg. range (kcal/mol
PBE	-2.37	2.69
B3LYP	-0.76	0.63
SCAN	-1.24	1.56
BLYP	-2.28	1.09

**Table 9:** DDEs (kcal/mol) for the RKT10 ( $\text{H}\cdots\text{H}\cdots\text{F}$ ) forward and reverse barriers using the three proxies  $^{13}$ , and a CCSD(T) reference  $^{14}$ . The proxies deviate significantly from the reference (by at least 1 kcal/mol) for each functional.

functional (barrier direction)	$\text{LC-}\omega\text{PBE}$	SX0.5	SCAN-FLOSIC	CCSD(T)
PBE (forward)	-1.31	-4.87	-6.44	-2.20
SCAN (forward)	-0.29	-2.52	-3.80	-1.00
PBE (reverse)	-1.11	-4.57	-5.45	-2.30
SCAN (reverse)	-0.22	-2.31	-3.15	-1.20

**Table 10:** Average and range of proxy DDEs  $^{13}$  (kcal/mol) of PBE and SCAN (Eq. 20) for four BH76 systems with significant disagreement between the proxies.

system	PBE (Avg / Range)	SCAN (Avg / Range)
$OH + N_2 \rightarrow N_2OH$ (ts)	-7.7 / 14.5	-5.5 / 11.2
$H + F_2 \rightarrow HF_2$ (ts)	-8.3 / 11.0	$-3.6 \ / \ 5.9$
$\mathrm{HF} + \mathrm{F} \to \mathrm{HF}_2 \; \mathrm{(ts)}$	-8.9 / 11.5	-4.4 / 6.7
$H_2 + PH_2 \rightarrow RKT12$	-8.2 / 21.6	-0.6 / 0.2

# V2. Unreliability of naive density-driven error interpolator

We now apply the lessons learned from previous sections to recent practical HF-DFT calculations in the literature which have led to so much confusion. We focus primarily on barrier heights, and in particular on  ${\rm H_2}+{\rm F}\to {\rm H}\cdots {\rm H}\cdots {\rm F}$  and an analog, as these have known densities and KS inversions. This system was studied in the context of DC-DFT by Kanungo et al.  $^{14}$ , wherein the NDI is used extensively. In this section, unless otherwise noted, we used CCSD(T) energy as  $E_v[n_v]$  while used KS inverted CCSD density as  $n_v({\bf r})$  to get pragmatic-DDE by using KS-pies  $^{71}$  code. Although CCSD(T) density should have been used for better accuracy, it was not done due to the significant computational cost of generating the density (Table S8 compares the total energy differences between CCSD and CCSD(T) densities for several atoms and anions and functionals, with differences less than 1 kcal/mol).

Begin with the unreliability of the NDI (Eq. 11) when applied inconsistently. Table 11 shows precisely the same patterns as we found in Table 4. Essentially any case where the NDI is applied to a density of a different functional gives a very wrong answer. To emphasize how dependent the numbers are on the choice of functional, we report the range (max minus min) of results for each given density; and we find that these errors are significant on the scale of the DDEs themselves. We also boldface the smallest NDI in each row. Again, we find no relation between the NDI and the true DDEs.

To ensure these are not accidental results of a given reaction, we repeat the process with  $H_2 + CI \rightarrow H \cdots H \cdots CI$  in Table 12. If you look at the values column-wise, we can see how different approximate functions evaluate the energy differently for the same density. No NDI consistently predicts the

**Table 11:** Matrix of naive density-driven error (DDE) interpolator (NDI) of Eq. 11 (in kcal/mol) for  $H_2 + F \rightarrow H \cdots H \cdots F$  reaction transition state, reactant, and barrier height. Green diagonals are (pragmatic-) DDEs. The range refers to the range of error predicted by the functionals for a given density. The bolded numbers indicate the density with the smallest NDI or for that functional.

					density			
	(kcal/mol)	SVWN	PBE	$r^2SCAN$	B3LYP	PBE0	$r^2 SCAN50$	$\text{LC-}\omega\text{PBE}$
				tı	ansition state			
	SVWN	-9.17	-7.10	-4.36	-5.36	-3.84	4.42	-4.53
-	PBE	-2.41	-4.45	-3.14	-3.64	-2.79	3.33	-2.89
functional	$r^2SCAN$	2.77	-0.51	-1.81	-1.23	-1.42	1.48	-0.83
cti	B3LYP	1.40	-1.43	-1.66	-2.24	-1.80	1.94	-1.74
£	PBE0	3.85	0.43	-0.85	-0.79	-1.23	1.10	-0.66
-	$r^2SCAN50$	11.52	6.39	1.74	2.61	0.72	-1.72	2.07
	$LC$ - $\omega PBE$	2.24	-0.50	-1.08	-1.56	-1.50	1.48	-2.07
	range	20.69	13.49	6.1	7.97	4.56	6.14	6.60
					reactant			
	SVWN	-4.14	-2.37	-0.66	-2.19	-1.25	1.80	-2.24
_	PBE	0.00	-1.76	-0.84	-1.59	-1.15	1.18	-1.51
functional	$r^2SCAN$	2.89	0.37	-0.56	0.02	-0.36	0.21	0.10
cţi	B3LYP	0.66	-1.11	-0.70	-1.29	-0.90	0.91	-1.04
g	PBE0	2.42	0.17	-0.26	-0.07	-0.46	0.46	0.00
	$r^2SCAN50$	5.49	2.52	0.26	1.70	0.40	-0.54	1.82
	$LC$ - $\omega PBE$	0.46	-1.17	-0.78	-1.19	-0.99	0.88	-1.44
	range	9.63	4.89	1.10	3.89	1.65	2.34	4.06
				ŀ	arrier height			
	SVWN	-5.03	-4.73	-3.70	-3.17	-2.59	2.62	-2.29
_	PBE	-2.41	-2.69	-2.30	-2.05	-1.64	2.15	-1.38
one	$r^2SCAN$	-0.12	-0.88	-1.25	-1.25	-1.06	1.27	-0.93
unctional	B3LYP	0.74	-0.32	-0.96	-0.95	-0.90	1.03	-0.70
Ę,	PBE0	1.43	0.26	-0.59	-0.72	-0.77	0.64	-0.66
-	$r^2SCAN50$	6.03	3.87	1.48	0.91	0.32	-1.18	0.25
	$\text{LC-}\omega\text{PBE}$	1.78	0.67	-0.30	-0.37	-0.51	0.60	-0.63
	range	11.06	8.60	5.18	4.08	2.91	3.80	2.54

**Table 12:** Same as Table 11, but with  $H_2 + Cl \rightarrow H \cdots H \cdots Cl$ .

	(1 1/ 1)	CININ	DDE	200131	density	DDEO	20043750	I.G. DDD
	(kcal/mol)	SVWN	PBE	r <sup>2</sup> SCAN	B3LYP	PBE0	r <sup>2</sup> SCAN50	$LC$ - $\omega PBE$
functional		transition state						
	SVWN	-5.60	-3.92	-0.88	-3.32	-1.89	3.11	-1.74
	PBE	-0.74	-2.39	-1.08	-1.99	-1.53	1.84	-0.78
	$r^2SCAN$	3.40	0.11	-1.19	0.08	-0.73	0.29	0.46
	B3LYP	0.23	-1.60	-0.72	-2.01	-1.38	1.17	-0.81
	PBE0	2.78	-0.02	-0.43	-0.26	-0.89	0.48	0.07
	$r^2SCAN50$	7.23	2.92	0.11	1.79	-0.05	-1.42	1.22
	$\text{LC-}\omega\text{PBE}$	1.44	-0.73	-0.78	-1.22	-1.49	0.13	-2.47
	range	12.83	6.84	1.30	5.11	1.84	4.53	3.69
		reactant						
	SVWN	-4.75	-3.22	-0.21	-3.1	-1.57	2.35	-2.42
_	PBE	-0.43	-1.94	-0.67	-1.74	-1.31	1.19	-1.30
functional	$r^2SCAN$	3.61	0.41	-0.87	0.36	-0.53	-0.13	0.15
	B3LYP	-0.24	-1.70	-0.65	-1.90	-1.32	0.82	-1.15
	PBE0	2.53	-0.02	-0.31	-0.08	-0.66	0.35	0.01
	$r^2SCAN50$	6.28	2.30	-0.18	1.83	0.10	-0.93	1.61
	$\text{LC-}\omega\text{PBE}$	0.46	-1.22	-0.88	-1.14	-1.23	0.58	-1.91
	range	11.03	5.52	0.70	4.93	1.67	3.28	4.03
		barrier height						
functional	SVWN	-0.85	-0.70	-0.67	-0.22	-0.32	0.76	0.68
	PBE	-0.31	-0.45	-0.41	-0.25	-0.22	0.65	0.52
	$r^2SCAN$	-0.21	-0.30	-0.32	-0.28	-0.20	0.42	0.31
	B3LYP	0.47	0.10	-0.07	-0.11	-0.06	0.35	0.34
	PBE0	0.25	0.00	-0.12	-0.18	-0.23	0.13	0.06
	$r^2SCAN50$	0.95	0.62	0.29	-0.04	-0.15	-0.49	-0.39
	$\text{LC-}\omega\text{PBE}$	0.98	0.49	0.10	-0.08	-0.26	-0.45	-0.56
	range	1.83	1.32	0.96	0.24	0.26	1.25	1.24

pragmatic-DDE. Even SVWN density has the smallest NDI among the 7 densities in some cases. This behavior occurs because each approximation samples and weights electron density differently across space, meaning that even visually similar densities can yield markedly different energies depending on the approximation employed. Therefore, it is not possible to infer density similarity from energy agreement, nor to evaluate the quality of a density based solely on its spatial resemblance to a reference. Discussing density quality outside the context of its self-consistent functional is meaningless. Conventional

density metrics based solely on spatial similarity are physically unfounded and potentially misleading for assessing density accuracy.

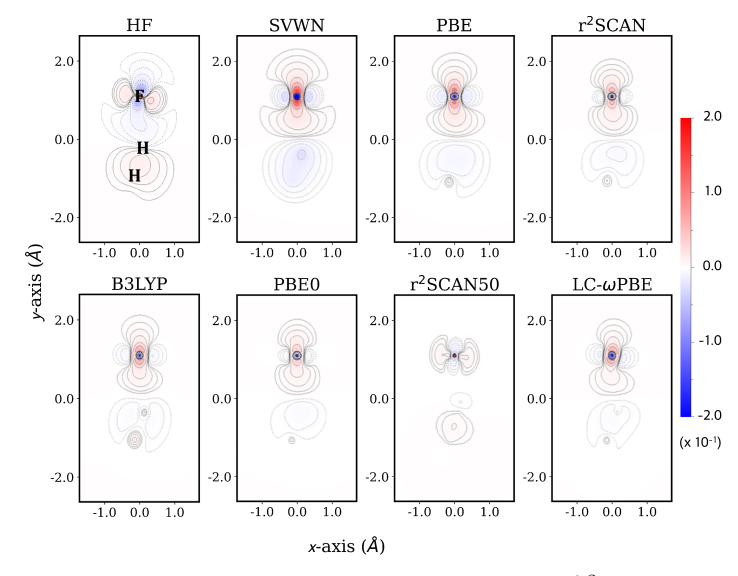


**Figure 14:** Contour maps of density errors  $(e/Å^3)$  for the  $H \cdots H \cdots F$  transition state, using CCSD as the reference. On this scale, CCSD and CCSD(T) appear identical (see Fig. S6).

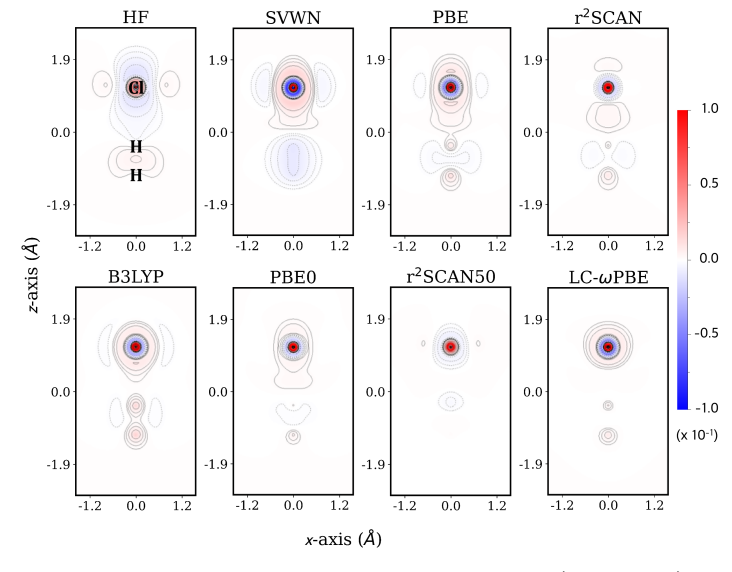


Figure 15: Same as Fig. 14, with F replaced by Cl (see Fig. S7).

Figure 14 is a density error contour map of the  $H\cdots H\cdots F$  transition state in the xy plane, while Fig. 15 repeats this for Cl in place of F. Visually, the HF, SVWN, PBE, r²SCAN , and B3LYP densities appear to be more different from the reference, while the densities of PBE0, r²SCAN50, and LC- $\omega$ PBE appear to be less different. In Refs. <sup>14</sup>, <sup>46</sup>, and <sup>61</sup>, they insist that the HF density is inaccurate because it looks spatially different from the density of the coupled-cluster methods. However, as noted in Ref. <sup>43</sup>, spatial differences in electron density do not directly imply improved accuracy, nor is the relationship between density errors and energy errors straightforward.

## V3. Proxy errors related to NDI errors

We have already seen that proxy benchmark densities introduced in the literature produce such a range of values that it undermines their credibility as proxies. We have also just documented how poorly the NDI performs when applied to any density other than its own self-consistent density, when it yields the DDE. In this section, we show that these two phenomena are intrinsically linked.

**Table 13:** Relationship between proxy DDE and the NDI, shown numerically for the forward RKT10 barrier height.  $\tilde{\mathcal{E}}$  values for LC- $\omega$ PBE were obtained from Ref. <sup>13</sup> (also presented in Table 9). Unit in kcal/mol.

functional	$n_{proxy}$	$\tilde{D}[n_{proxy}]$	$\mathcal{\tilde{E}}[n_{proxy}]$	DDE
PBE	$\text{LC-}\omega\text{PBE}$	-1.38	-1.31	-2.69
PBE	$\rm r^2SCAN50$	2.15	-4.85	-2.69
SCAN	$\text{LC-}\omega\text{PBE}$	-0.95	-0.29	-1.24
SCAN	$r^2SCAN50$	1.28	-2.50	-1.24

The proxy DDE  $\tilde{\mathcal{E}}_D$  and the naive interpolator  $\tilde{D}$  follow an exact relationship. For a given proxy density, and approximate functional, adding together Eqs. 11 and 20 gives:

$$\widetilde{\mathcal{E}}_D[n_{proxy}] = \Delta \widetilde{E}_D - \widetilde{D}[n_{proxy}]$$
 (21)

This is illustrated in Table 13. But the interpretation is very interesting. If the proxy benchmark were close to the exact density,  $D[n_{proxy}]$  would be much smaller than DDE, and  $\mathcal{E}_D$ would be close to DDE. We clearly see that this is not true for the crucial case of  $H_2 + F \rightarrow H \cdots H \cdots F$ , the one case where a sufficiently accurate density was found and inversion could be done. In every case, the benchmark proxy density yields a terrible estimate of the DDE. We can now relate the failure of proxy benchmarks to the overestimates of NDI. If a proxy benchmark density is close to the exact density, its ideal DDE is very small, and vanishes quadratically as the exact density is approached. But our formula has  $\widetilde{D}[n_{proxy}]$  instead, which is linear in the difference, and much larger than the ideal DDE. But the larger it is, the more inaccurate the proxy density is for estimating the DDE. The benchmark proxies would need to be extremely close to exact in order to make this difference negligible, and none of those suggested or being used in the literature meet this criterion.

### V4. Analysis in terms of total energies

In this last section, we work backwards and decompose the errors in chemical reaction energies into their total energy components, such as the transition state and the reactants in the case of a barrier height. Although density functional approximations often yield large absolute errors in total energies due to intrinsic limitations when their functional forms are applied to core electrons, they are nonetheless highly effective

in predicting relative quantities such as reaction energies and barriers. The errors in total energies are often much larger than the energy difference itself, and vary enormously among different approximate functionals. The reliability for energy differences largely stems from a systematic cancellation of FEs: when the energetic errors of the reactants and products are of comparable magnitude, their difference—the relative energy—remains accurate even if the respective errors are significant.

As stated repeatedly above, unfortunately, we cannot directly measure the HF-DFT's DDE, or even have a good estimate. What we can do is calculate the pragmatic DDE of self-consistent functionals when we can calculate accurate densities and perform sufficiently accurate KS-inversions. Figure 16 presents the distribution of the ratio of the product DDE divided by the reactant DDE for 103 benchmark reactions. (See Table S9 for a complete list of reactions selected based on whether they were small enough to allow CCSD density calculations in the GMTKN55 and Bauzá30<sup>72</sup> datasets.) If the DDE of the reactant and product are similar, their values in the energy difference will cancel each other out and will not affect the overall error. In the density-insensitive case, the distribution of ratios is relatively clustered around 1. However, in the density-sensitive case, the ratios are distributed far from 1. It is clear that the difference in error between reactant and product mentioned affects DDE as in Table 11. A few outliers far from 1 in density-insensitive cases may look quite strange, but this occurs only because the reactant DDE in the denominator is very small (see the number next to the marker).

## V5. Relationships between density-driven errors and standard metrics of density errors

Quantitatively assessing the accuracy of an electron density is inherently challenging. The DFT literature is full of density error plots and many different metrics to measure density differences. In fact, one can devise infinitely many such measures, and different ones are used to make different points. Some show self-consistent densities to be preferable, others find HF densities better.

An important point to note is that, for spatially open-shell cases, there is freedom in the orientation of the orbitals, which must be accounted for when calculating the error. This occurs for some commonly used metrics, such as the  $L_2$  norm or differences in Coulomb self-energy. For systems with degenerate electronic configurations, the orientation and occupation of atomic or molecular orbitals can vary arbitrarily without affecting observable properties such as energies. Figure 17 illustrates this point: Due to the degeneracy of the O atom's 2p orbitals, electron densities computed using the same functional (e.g., PBE) may differ in shape. In such cases, direct comparison of real-space densities becomes unreliable, even

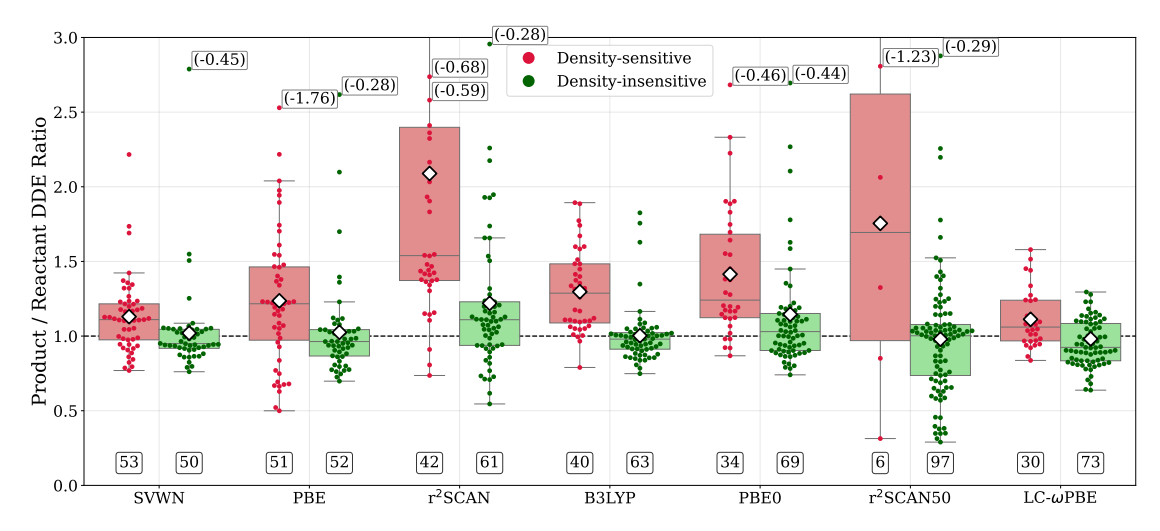


Figure 16: Distributions of the ratio of density-driven error (DDE) between product and reactant for 103 benchmark reaction energies (see Table S9 for the full list). Reactions are categorized as density-sensitive (red) or density-insensitive (green). The number below each box indicates the number of reactions included in that category. White diamond markers denote the mean DDE ratio within each box. For cases where the ratio exceeds 2.5, the corresponding value in parentheses indicates the DDE of the reactant (in kcal/mol). In density-insensitive reactions, the DDE ratio is generally clustered around 1, indicating similar DDE contributions from both reactants and products. In contrast, density-sensitive reactions exhibit larger deviations from 1, suggesting significant differences in DDE between reactant and product. These results support the view that DDE contributes to energy errors primarily in density-sensitive cases, highlighting a link between DDE magnitude and density sensitivity.

when the densities are obtained using the identical method, unless this ambiguity is removed. As a result, spatial features of the electron density may differ in ways that are not physically significant, thereby confounding numerical comparisons. This degeneracy-related variability in real-space density distributions can lead to misleading conclusions when comparing electron densities across different calculations or methods.

To avoid spatial ambiguities—such as the orbital occupation variability illustrated in Fig. 17—a subset of 36 reactions was selected from the 103 benchmark reactions in Table S9 (see the reaction index that marked with an asterisk in Table S9). Only reactions involving closed-shell or non-degenerate open-shell species were included, allowing for reliable correlation analysis between DDE and real-space density metrics. This subset avoids artifacts arising from arbitrary orbital occupations in degenerate systems. Figure 18 presents the relationship between DDE and the  $L_2$  norm of the density difference for this subset, evaluated across nine approximate functionals and HF. As previously noted, establishing a clear and quantitative relationship between real-space density features and DDE remains challenging. Indeed, little to no correlation is observed between DDE and density error metrics such as the  $L_1$ ,  $L_2$  norms, Shannon entropy  $^{73}$ , Fisher information  $^{74}$ , and Coulomb self-energy (see Figs. S9-S18). Despite extensive attempts, we failed to find any such correlation, nor have we identified any in the literature.

#### VI. DISCUSSION AND RECENT LITERATURE

To explain the significance of our findings to work in the literature, we consider specifically the barrier height of  $H_2+F\to H\cdots H$  (and its backward reaction) as it plays a crucial role in propagating confusion about DDEs. An earlier paper appeared to show, using proxy densities and the NDI, that there were larger DDEs in HF-DFT than DFT, hence suggesting a cancellation of errors between DDE and FE is responsible for the improved performance of HF-DFT for barrier heights. In Ref.  $^{14}$ , one specific case was targeted for finding an accurate density and KS inversion, as a check on the value of the proxies.

Table 1 of that work reports barrier heights for that reaction, both forwards and backwards. We already showed in Sec. V1 that the proxy densities are far too inaccurate to be useful for these purposes (see Table 8). We also note that all the reports of DDEs for HF-DFT should be discarded, as these are actually NDIs on non-self-consistent densities. It is unknown how large the DDE for those calculations is.

But there is a crucial trend not pointed out in the paper. For every single case (7 functionals times two barrier heights), the change in barrier height from the self-consistent result to the HF-DFT result is in the same direction as the change from self-consistent to exact. Compare this with our Fig. 1 for one-electron systems, parameterized by a. Here, we do not have all densities along one line. The HF density is in some

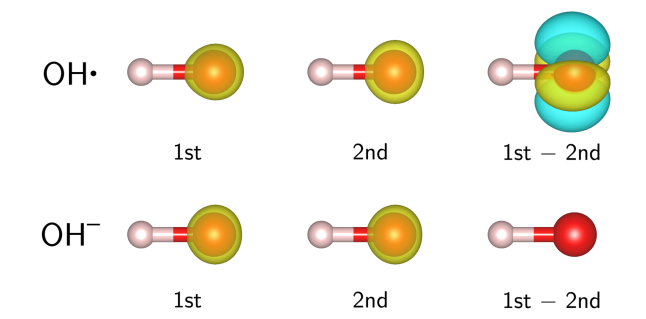


Figure 17: Electron densities and their differences between two independent PBE calculations (1st and 2nd) for the OH radical (top row) and the OH<sup>-</sup> anion (bottom row). The OH radical exhibits substantial density variations due to degeneracyinduced random orbital occupations resulting from different selfconsistent field convergence paths, whereas the closed-shell OH<sup>-</sup> anion shows minimal differences. Yellow and cyan isosurfaces indicate positive and negative density differences, respectively. The isosurface level is set to 0.7 for individual molecular densities and 0.03 for the density differences. Quantitative comparisons of the 1st and 2nd densities for each molecule using known real-space density metrics yield the following values (in the order of OH radical, OH<sup>-</sup> anion):  $L_1 = (1.2, 2.0 \times 10^{-6}), L_2 =$  $(0.32, 4.0 \times 10^{-7})$ , Shannon entropy =  $(2.0, 6.0 \times 10^{-6})$ , Fisher information =  $(12.6, 2.0 \times 10^{-5})$ , and Coulomb self-energy =  $(0.06, 3.0 \times 10^{-13})$ . (See Figs. S9–S18 for the definitions of each metric.)

other 'direction' in density space. But the results are perfectly consistent with Fig. 1. It looks like the HF-DFT density is much closer to the exact density than the self-consistent one is, which suggests strongly that its DDE, if we could measure it, would be smaller in magnitude than that of each of the functionals. Note that it would change from one functional to the next, but should be far less than the numbers reported in the paper. Lastly, we note that the FE for each functional is typically larger in magnitude than the TE on the HF density, which excludes the naive interpretation of DC-DFT. <sup>13–16,75</sup> But this is just like Fig. 1, on the right. There's a range of densities that are more accurate than the self-consistent density, but with errors less than the FE. Both the DDE and FE are reduced by moving to the HF density. This is an automatic consequence of the (near) parabolic shape of the approximate functional with minimum at the self-consistent density. The naive explanation applies to the left hand side, but the righthand side exists also. Thus, the tremendous improvement in barrier height with HF-DFT does not contradict the principles of DC-DFT. The real question is whether the DDE of such a calculation is bigger or smaller than that of the self-consistent calculation, a question we are currently unable to answer.

Table 14 gives a list of appearances of the three major sources of confusion introduced in the recent literature about DC-DFT: using NDI to decide the DDE of HF-DFT calculations, use of proxies as benchmark densities when they are not

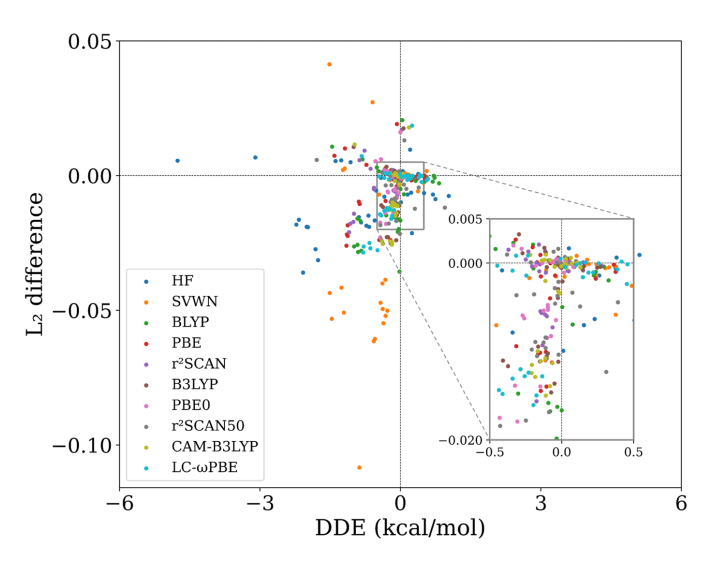


Figure 18: Relation between density-driven error (DDE) and  $L_2$  norm differences for the 36 selected reactions (listed in Table S9), evaluated across various density functionals. CCSD densities are used as the reference. (See Figs. S9–S18 for additional comparisons using other density metrics, including  $L_1$  norm, Shannon entropy, Fisher information, and Coulomb self-energy.)

sufficiently accurate, and the idea that 'natural' metrics, such as the  $L_2$  norm, for density errors can somehow be correlated with the measures used in DC-DFT.

**Table 14:** Appearance in recent literature of the naive density-driven error interpolator (NDI), proxy benchmark densities, and scalar measures of density differences.

NDI				
Nam $2020^{12}$	Fig. 2, Fig. 4			
Kaplan $2023^{13}$	Eq. 11, Table 5			
Kanungo $2024^{14}$	Eq. 4, Table 1, Table 2			
Kaplan $2024^{15}$	Eq. 11, Fig. 1, Fig. 3, Fig. 4, Fig. 5			
Pangeni $2025^{16}$	Eq. 4, Table 2			
proxy benchmark densities				
Kaplan 2023 13	Eq. 10, Eq. 11, Table 5			
Kanungo $2024^{14}$	Table 2			
Kaplan $2024^{15}$	Eq. 6			
metrics of density difference				
Medvedev 2017 <sup>46</sup>	Fig. 1, Fig. 2, Table 1			
Dasgupta $2022^{34}$	Eq. 9 ,Fig. 7			
Shahi 2025 <sup>61</sup>	Eq. 1			

#### VII. CONCLUSIONS

There are many lessons to be drawn from the results presented here, lessons that are important for understanding how DC-DFT works. First, *any* work using the naive density-driven error (DDE) interpolator (NDI) yields essentially no quantitative information about DDEs, and our results suggest it likely

hugely overestimates DDEs. As far as we know, there are no reliable estimates of DDEs for HF-DFT (apart from those here), and there is no evidence in the literature that the HF density is less accurate than a typical self-consistent density (using the only measure that is relevant to DC-DFT). Claims of unusual or unexplained cancellations of errors between DDEs and functional errors (FE) should be discounted. Our results suggest that actual DDEs of HF-DFT densities are likely much smaller than those reported, leaving no significant cancellation of errors. Moreover, the densities of HF-DFT calculations may be quite different from HF densities themselves. Finally, our results show that under typical circumstances, it is not surprising that often the energy error using the HF density is lower than the energy of the exact density (the FE), and that such cases can easily occur even when the HF density is more accurate than the self-consistent density.

Two further points are worth emphasizing. First, one must be extremely careful before using proxies in place of benchmark densities. In general, if the proxy does not come from a self-consistent KS calculation, we have no reliable way to estimate its density-driven error. Even if it does, and we can calculate its DDE, this is not a definitive yardstick for comparing one functional's density to another's, as the DDE depends on the functional chosen. For reasonably accurate functionals, our examples show that these are usually good proxies for ideal-DDEs, which can be compared directly (but require knowledge of the exact functional to calculate directly). Even a very small pragmatic-DDE cannot be taken as definitive evidence that the density is intrinsically accurate, and proxy densities may be too unreliable for estimating ideal-DDEs or for preserving the correct relative ordering of DDEs across standard functionals. Second, there are endless interesting measures of the 'accuracy' of a density, from  $L_2$  norms to kinetic energies to Shannon entropies. We have searched hard, and found none that correlate with the DDEs defined in DC-DFT. There are two simple reasons for this. First, DC-DFT is applied to the energy differences that are the relevant quantities in materials and quantum chemistry. There is rarely an obvious route to applying some norm over a density to differences in densities. Second, DDEs depend on the entire functionals in an extremely complex way, so that it is unsurprising that their patterns are difficult to capture by focusing on just one single measure. Thus it seems always a mistake to conflate small density errors by one of these metrics with small ideal DDEs.

Calculation of (pragmatic-)DDE for a given self-consistent DFT calculation and energy difference is straightforward when a benchmark energy and density is available, provided they are sufficiently accurate. But this requires that the functional be applied self-consistently, which is not the case for HF-DFT. To find out if the HF density is more accurate by the measure of DC-DFT, requires evaluation of the exact functional on an approximate density. In general, this is impossible with

present computational techniques, except for the simple cases presented here. Thus, for practical cases such as barrier heights, we cannot definitively quantify the DDE of the HF density. But we can say that all previous attempts to do so, based on the NDI, should be discounted, leaving no evidence that the HF density is less accurate than the self-consistent density in cases where it matters (density-sensitive cases). In any event, the discussion is largely misplaced, as the density of HF-DFT is not the HF density.

However, what is clear is that the case of barrier heights does not fit the same mold as other known successes of HF-DFT. For example, for dissociation curves, it has been shown that the density-driven error dominates in the large separation limit, and that the HF density is far better than the self-consistent density in that limit, and so almost entirely eliminates the error. 8 Neither of these statements apply to barrier heights (and perhaps other situations, too). Both existing literature 13-16,75 and our own calculations clearly show that density driven errors of self-consistent calculations do not dominate the errors in barrier heights, and that the improvements typically rendered by HF-DFT are significantly larger in magnitude than the density-driven error. It is plausible that the true density of an HF-DFT calculation (which is not the HF density) is more accurate (i.e., has a lower ideal DDE than the self-consistent density), as in our one-electron examples of Sec. IV1. But that would not alter the fact that the dominant improvement is in the functional-driven error, which is consistently significantly smaller than its self-consistent counterpart. When exact density (here, CCSD or CCSD(T)) is evaluated on approximate functionals, the (pragmatic-)DDE vanishes, leaving only the FE. Our DC-DFT analysis explains how HF-DFT can achieve lower errors than functional errors, but not why it so consistently improves barriers. Given the mild increase in multireference character of the transition state relative to reactants, it also cannot be ruled out that CCSD yields densities (not energies) that are insufficiently accurate on the scale needed for DC-DFT analysis.

The bottom line of this work is that we have corrected several errors in the literature, and performed a thorough DC-DFT analysis of the case of barrier heights, to the extent that is currently possible. Almost all existing evidence in the literature for the size of DDEs of HF-DFT and significant cancellations of errors between FE and DDE is marred by the use of the unreliable DDE interpolator (or use of proxies), and all conclusions based on those numbers about the sizes of DDEs of HF-DFT should be discounted. Moreover, the success of HF-DFT for barrier heights (and other cases) can still be understood within DC-DFT, by noting that an energy error in HF-DFT that is less than the FE is not unexpected. Regardless of the relative accuracy of the HF density (which depends mightily on how you measure it), the density of an HF-DFT calculation is not the HF density. In the one case

where we could easily find that density, the corresponding functional has both smaller DDE's and FE's than the original. This explains how HF-DFT can yield smaller errors than the FE of the original functional, but sadly does not explain why it reduces most FEs of most semilocal functionals by so much. It seems likely that further insight, combined with DC-DFT analysis, is needed.

## COMPUTATIONAL DETAILS

The aug-cc-pV5Z  $^{76}$  basis set is used for every energy and density calculations. All HF, DFT, and coupled-cluster calculations in this paper were done by PySCF  $^{77,78}$  2.9.0 version, except Figs. 8, 14, and 15, which used ORCA  $^{79-81}$  6.0.1 version and Multiwfn  $^{82,83}$  to draw density contour map. Figure 17 is drawn by VESTA  $^{84}$ . We set NoFrozencore option for coupled-cluster calculation in ORCA. For Kohn-Sham inversion, we use the Zhao-Morisson-Parr (ZMP)  $^{62}$  algorithm in KS-pies  $^{71}$  package and set 1024 for maximal  $\lambda$  and used Fermi-Amaldi (FA)  $^{85}$  for the guiding potential.

#### Supporting Information

Geometries for one-electron systems, Energy curves of one-electron systems, Error distribution of DFT and HF-DFT for 103 benchmark reactions, Table of energy difference between CCSD and CCSD(T) densities, Table of subset, systems, and stoichiometry information for the 103 benchmark reactions, Table of reaction indices of the 36 selected non-degenerated reactions, Table of ideal-DDE, pragmatic-DDE, and NDI of one-electron systems, Figures of density difference contour map between CCSD and CCSD(T), Figures of relationship between DDE and real-space density metrics, Raw data of density-sensitivity, DFT, HF-DFT, coupled-cluster, and total energies for whole density-functional combinations (in XLSX).

### ACKNOWLEDGMENTS

We are grateful for the support of the National Research Foundation of Korea (NRF-RS-2025-00554671) and the Korea Environment Industry & Technology Institute (KEITI-RS-2023-00219144). S.C. acknowledges support from the UC Presidential Dissertation Year fellowship (PDY). K.B. acknowledges support from NSF grant No.CHE-2154371.

#### References

- (1) Kohn, W.; Sham, L. J. Self-consistent equations including exchange and correlation effects. *Physical review* **1965**, *140*, A1133.
- (2) Kim, M.-C.; Sim, E.; Burke, K. Understanding and reducing errors in density functional calculations. *Phys. Rev. Lett.* **2013**, *111*, 073003.
- (3) Slater, J. C. A simplification of the Hartree-Fock method. *Phys. Rev.* **1951**, *81*, 385.
- (4) Goerigk, L.; Hansen, A.; Bauer, C.; Ehrlich, S.; Najibi, A.; Grimme, S. A look at the density functional theory zoo with the advanced GMTKN55 database for general main group thermochemistry, kinetics and noncovalent interactions. *Phys. Chem. Chem. Phys.* 2017, 19, 32184–32215.
- (5) Song, S.; Vuckovic, S.; Sim, E.; Burke, K. Density sensitivity of empirical functionals. J. Phys. Chem. Lett. 2021, 12, 800–807.
- (6) Santra, G.; Martin, J. M. What types of chemical problems benefit from density-corrected DFT? A probe using an extensive and chemically diverse test suite. *J. Chem. Theory Comput.* **2021**, *17*, 1368–1379.
- (7) Yu, H.; Song, S.; Nam, S.; Burke, K.; Sim, E. Density-corrected density functional theory for open shells: How to deal with spin contamination. *J. Phys. Chem. Lett.* 2023, 14, 9230–9237.
- (8) Lee, M.; Kim, B.; Sim, M.; Sogal, M.; Kim, Y.; Yu, H.; Burke, K.; Sim, E. Correcting dispersion corrections with density-corrected DFT. *J. Chem. Theory Comput.* **2024**, *20*, 7155–7167.
- (9) Kim, Y.; Sim, M.; Lee, M.; Kim, S.; Song, S.; Burke, K.; Sim, E. Extending density-corrected density functional theory to large molecular systems. *J. Phys. Chem. Lett.* **2024**, *16*, 939–947.
- (10) Zhang, Y.; Yang, W. A challenge for density functionals: Self-interaction error increases for systems with a noninteger number of electrons. J. Chem. Phys. 1998, 109, 2604–2608.
- (11) Kim, M.-C.; Sim, E.; Burke, K. Ions in solution: Density corrected density functional theory (DC-DFT). *J. Chem. Phys.* **2014**, *140*.
- (12) Nam, S.; Song, S.; Sim, E.; Burke, K. Measuring density-driven errors using Kohn–Sham inversion. *J. Chem. Theory Comput.* **2020**, *16*, 5014–5023.

- (13) Kaplan, A. D.; Shahi, C.; Bhetwal, P.; Sah, R. K.; Perdew, J. P. Understanding density-driven errors for reaction barrier heights. *J. Chem. Theory Comput.* **2023**, *19*, 532–543.
- (14) Kanungo, B.; Kaplan, A. D.; Shahi, C.; Gavini, V.; Perdew, J. P. Unconventional error cancellation explains the success of Hartree–Fock density functional theory for barrier heights. J. Phys. Chem. Lett. 2024, 15, 323–328.
- (15) Kaplan, A. D.; Shahi, C.; Sah, R. K.; Bhetwal, P.; Kanungo, B.; Gavini, V.; Perdew, J. P. How does HF-DFT achieve chemical accuracy for water clusters? *J. Chem. Theory Comput.* 2024, 20, 5517–5527.
- (16) Pangeni, N.; Shahi, C.; Perdew, J. P.; Subramanian, V.; Kanungo, B.; Gavini, V.; Ruzsinszky, A. Hartree-Fock density functional theory works through error cancellation for the interaction energies of halogen and chalcogen bonded complexes. *ChemRxiv* 2025, Preprint, https: //doi.org/10.26434/chemrxiv-2025-wfft9.
- (17) MacDonald, J. Successive approximations by the Rayleigh-Ritz variation method. *Phys. Rev.* **1933**, *43*, 830.
- (18) Lieb, E. H. Density functionals for Coulomb systems. *Int. J. Quantum Chem.* **1983**, *24*, 243–277.
- (19) Von Barth, U.; Hedin, L. A local exchange-correlation potential for the spin polarized case. i. *J. Phys. C: Solid State Phys.* **1972**, *5*, 1629.
- (20) Vuckovic, S.; Song, S.; Kozlowski, J.; Sim, E.; Burke, K. Density functional analysis: The theory of densitycorrected DFT. J. Chem. Theory Comput. 2019, 15, 6636–6646.
- (21) Hernandez, D. J.; Rettig, A.; Head-Gordon, M. A New View on Density Corrected DFT: Can One Get a Better Answer for a Good Reason? arXiv preprint arXiv:2306.15016 2023,
- (22) Sim, E.; Song, S.; Vuckovic, S.; Burke, K. Improving results by improving densities: Density-corrected density functional theory. *J. Am. Chem. Soc.* **2022**, *144*, 6625–6639.
- (23) Gill, P. M.; Johnson, B. G.; Pople, J. A.; Frisch, M. J. An investigation of the performance of a hybrid of Hartree-Fock and density functional theory. *International Journal of Quantum Chemistry* **1992**, *44*, 319–331.
- (24) Oliphant, N.; Bartlett, R. J. A systematic comparison of molecular properties obtained using Hartree–Fock, a hybrid Hartree–Fock density-functional-theory, and coupledcluster methods. J. Chem. Phys. 1994, 100, 6550–6561.

- (25) Janesko, B. G.; Scuseria, G. E. Hartree–Fock orbitals significantly improve the reaction barrier heights predicted by semilocal density functionals. J. Chem. Phys. 2008, 128.
- (26) Verma, P.; Perera, A.; Bartlett, R. J. Increasing the applicability of DFT I: Non-variational correlation corrections from Hartree–Fock DFT for predicting transition states. *Chem. Phys. Lett.* 2012, 524, 10–15.
- (27) Rana, B.; Coons, M. P.; Herbert, J. M. Detection and correction of delocalization errors for electron and hole polarons using density-corrected DFT. *J. Phys. Chem. Lett.* **2022**, *13*, 5275–5284.
- (28) Nam, S.; Cho, E.; Sim, E.; Burke, K. Explaining and fixing DFT failures for torsional barriers. *J. Phys. Chem. Lett.* **2021**, *12*, 2796–2804.
- (29) Kim, Y.; Song, S.; Sim, E.; Burke, K. Halogen and chalcogen binding dominated by density-driven errors. *J. Phys. Chem. Lett.* **2018**, *10*, 295–301.
- (30) Bryenton, K. R.; Adeleke, A. A.; Dale, S. G.; Johnson, E. R. Delocalization error: The greatest outstanding challenge in density-functional theory. *Wiley Interdisciplinary Reviews: Computational Molecular Science* **2023**, *13*, e1631.
- (31) Kim, M.-C.; Sim, E.; Burke, K. Communication: Avoiding unbound anions in density functional calculations. *J. Chem. Phys.* **2011**, *134*.
- (32) Kim, M.-C.; Park, H.; Son, S.; Sim, E.; Burke, K. Improved DFT potential energy surfaces via improved densities. *J. Phys. Chem. Lett.* **2015**, *6*, 3802–3807.
- (33) Dasgupta, S.; Lambros, E.; Perdew, J. P.; Paesani, F. Elevating density functional theory to chemical accuracy for water simulations through a density-corrected manybody formalism. *Nat. Commun.* 2021, 12, 6359.
- (34) Dasgupta, S.; Shahi, C.; Bhetwal, P.; Perdew, J. P.; Paesani, F. How good is the density-corrected SCAN functional for neutral and ionic aqueous systems, and what is so right about the Hartree–Fock density? *J. Chem. Theory Comput.* **2022**, *18*, 4745–4761.
- (35) Palos, E.; Lambros, E.; Dasgupta, S.; Paesani, F. Density functional theory of water with the machine-learned DM21 functional. *J. Chem. Phys.* **2022**, *156*.
- (36) Palos, E.; Caruso, A.; Paesani, F. Consistent density functional theory-based description of ion hydration through density-corrected many-body representations. *J. Chem. Phys.* **2023**, *159*.

- (37) Song, S.; Vuckovic, S.; Kim, Y.; Yu, H.; Sim, E.; Burke, K. Extending density functional theory with near chemical accuracy beyond pure water. *Nat. Commun.* **2023**, *14*, 799.
- (38) Belleflamme, F.; Hutter, J. Radicals in aqueous solution: assessment of density-corrected SCAN functional. *Phys. Chem. Chem. Phys.* **2023**, *25*, 20817–20836.
- (39) Broderick, D. R.; Herbert, J. M. Delocalization error poisons the density-functional many-body expansion. *Chem. Sci.* 2024, 15, 19893–19906.
- (40) Zhang, J.; Pagotto, J.; Gould, T.; Duignan, T. T. Scalable and accurate simulation of electrolyte solutions with quantum chemical accuracy. *Mach. Learn. Sci. Technol.* **2025**,
- (41) Rana, B.; Beran, G. J.; Herbert, J. M. Correcting  $\pi$ -delocalisation errors in conformational energies using density-corrected DFT, with application to crystal polymorphs. *Mol. Phys.* **2023**, *121*, e2138789.
- (42) Morgante, P.; Autschbach, J. Density-corrected density functional theory for molecular properties. *J. Phys. Chem. Lett.* **2023**, *14*, 4983–4989.
- (43) Sim, E.; Song, S.; Burke, K. Quantifying density errors in DFT. *J. Phys. Chem. Lett.* **2018**, *9*, 6385–6392.
- (44) Martín-Fernández, C.; Harvey, J. N. On the use of normalized metrics for density sensitivity analysis in dft. J. Phys. Chem. A 2021, 125, 4639–4652.
- (45) Graf, D.; Thom, A. J. Simple and efficient route toward improved energetics within the framework of density-corrected density functional theory. *J. Chem. Theory Comput.* **2023**, *19*, 5427–5438.
- (46) Medvedev, M. G.; Bushmarinov, I. S.; Sun, J.; Perdew, J. P.; Lyssenko, K. A. Density functional theory is straying from the path toward the exact functional. *Science* **2017**, *355*, 49–52.
- (47) Wagner, L. O.; Stoudenmire, E. M.; Burke, K.; White, S. R. Guaranteed convergence of the kohn-sham equations. *Phys. Rev. Lett.* **2013**, *111*, 093003.
- (48) Furness, J. W.; Kaplan, A. D.; Ning, J.; Perdew, J. P.; Sun, J. Accurate and numerically efficient r2SCAN metageneralized gradient approximation. J. Phys. Chem. Lett. 2020, 11, 8208–8215.
- (49) Stephens, P. J.; Devlin, F. J.; Chabalowski, C. F.; Frisch, M. J. Ab initio calculation of vibrational absorption and circular dichroism spectra using density functional force fields. J. Phys. Chem. 1994, 98, 11623–11627.

- (50) Perdew, J. P.; Burke, K.; Ernzerhof, M. Generalized gradient approximation made simple. *Phys. Rev. Lett.* **1996**, 77, 3865.
- (51) Becke, A. D. Density-functional exchange-energy approximation with correct asymptotic behavior. *Phys. Rev. A.* 1988, 38, 3098.
- (52) Lee, C.; Yang, W.; Parr, R. G. Development of the Colle-Salvetti correlation-energy formula into a functional of the electron density. *Phys. Rev. B.* 1988, 37, 785.
- (53) Dirac, P. A. M. Note on Exchange Phenomena in the Thomas Atom. *Math. Proc. Camb. Philos. Soc.* **1930**, *26*, 376–385.
- (54) Vosko, S. H.; Wilk, L.; Nusair, M. Accurate spindependent electron liquid correlation energies for local spin density calculations: a critical analysis. *Can. J. Phys.* 1980, 58, 1200–1211.
- (55) Bursch, M.; Neugebauer, H.; Ehlert, S.; Grimme, S. Dispersion corrected r2SCAN based global hybrid functionals: r2SCANh, r2SCAN0, and r2SCAN50. *J. Chem. Phys.* **2022**, *156*.
- (56) Vydrov, O. A.; Scuseria, G. E. Assessment of a longrange corrected hybrid functional. J. Chem. Phys. 2006, 125.
- (57) Yanai, T.; Tew, D. P.; Handy, N. C. A new hybrid exchange–correlation functional using the Coulombattenuating method (CAM-B3LYP). *Chem. Phys. Lett.* **2004**, *393*, 51–57.
- (58) Perdew, J. P.; Ernzerhof, M.; Burke, K. Rationale for mixing exact exchange with density functional approximations. J. Chem. Phys. 1996, 105, 9982–9985.
- (59) Szabo, A.; Ostlund, N. Modern Quantum Chemistry: Introduction to Advanced Electronic Structure Theory; Dover Books on Chemistry; Dover Publications, 1996.
- (60) Görling, A.; Levy, M. Correlation-energy functional and its high-density limit obtained from a coupling-constant perturbation expansion. *Physical Review B* 1993, 47, 13105.
- (61) Shahi, C.; Perdew, J. P. Comment on "Accurate Correlation Potentials from the Self-Consistent Random Phase Approximation". Phys. Rev. Lett. 2025, 135, 019601.
- (62) Zhao, Q.; Morrison, R. C.; Parr, R. G. From electron densities to Kohn-Sham kinetic energies, orbital energies, exchange-correlation potentials, and exchange-correlation energies. *Phys. Rev. A.* 1994, 50, 2138.

- (63) Wu, Q.; Yang, W. A direct optimization method for calculating density functionals and exchange–correlation potentials from electron densities. J. Chem. Phys. 2003, 118, 2498–2509.
- (64) Shi, Y.; Wasserman, A. Inverse Kohn–Sham density functional theory: Progress and challenges. 2021, 12, 5308– 5318.
- (65) Gould, T. Toward routine Kohn–Sham inversion using the "Lieb-response" approach. J. Chem. Phys. **2023**, 158.
- (66) Callow, T. J.; Lathiotakis, N. N.; Gidopoulos, N. I. Density-inversion method for the Kohn–Sham potential: Role of the screening density. J. Chem. Phys. 2020, 152.
- (67) Erhard, J.; Trushin, E.; Görling, A. Numerically stable inversion approach to construct Kohn–Sham potentials for given electron densities within a Gaussian basis set framework. J. Chem. Phys. 2022, 156.
- (68) Erhard, J.; Trushin, E.; Görling, A. Kohn–Sham inversion for open-shell systems. *J. Chem. Phys.* **2025**, *162*.
- (69) Takahashi, H. Comparison of optimized effective potential with inverse Kohn–Sham method for Hartree–Fock exchange energy. J. Chem. Phys. 2024, 161.
- (70) Kanungo, B.; Zimmerman, P. M.; Gavini, V. Exact exchange-correlation potentials from ground-state electron densities. *Nat. Commun.* 2019, 10, 4497.
- (71) Nam, S.; McCarty, R. J.; Park, H.; Sim, E. KS-pies: Kohn–Sham inversion toolkit. *J. Chem. Phys.* **2021**, *154*.
- (72) Bauza, A.; Alkorta, I.; Frontera, A.; Elguero, J. On the reliability of pure and hybrid DFT methods for the evaluation of halogen, chalcogen, and pnicogen bonds involving anionic and neutral electron donors. J. Chem. Theory Comput. 2013, 9, 5201–5210.
- (73) Shannon, C. E. A mathematical theory of communication. *Bell Syst. Tech. J.* **1948**, *27*, 379–423.
- (74) Fisher, R. A. Theory of Statistical Estimation. *Math. Proc. Camb. Philos. Soc.* **1925**, *22*, 700–725.
- (75) Wibowo-Teale, A. M.; Huynh, B. C.; Helgaker, T.; Tozer, D. J. Classical reaction barriers in dft: an adiabaticconnection perspective. *J. Chem. Theory Comput.* 2024, 21, 124–137.
- (76) Dunning Jr, T. H. Gaussian basis sets for use in correlated molecular calculations. I. The atoms boron through neon and hydrogen. J. Chem. Phys. 1989, 90, 1007–1023.

- (77) Sun, Q.; Berkelbach, T. C.; Blunt, N. S.; Booth, G. H.; Guo, S.; Li, Z.; Liu, J.; McClain, J. D.; Sayfutyarova, E. R.; Sharma, S.; others PySCF: the Pythonbased simulations of chemistry framework. Wiley Interdisciplinary Reviews: Computational Molecular Science 2018, 8, e1340.
- (78) Sun, Q.; Zhang, X.; Banerjee, S.; Bao, P.; Barbry, M.; Blunt, N. S.; Bogdanov, N. A.; Booth, G. H.; Chen, J.; Cui, Z.-H.; others Recent developments in the PySCF program package. J. Chem. Phys. 2020, 153.
- (79) Neese, F. The ORCA program system. *Wiley Interdiscip. Rev.: Comput. Mol. Sci.* **2012**, *2*, 73–78.
- (80) Neese, F. Software update: the ORCA program system, version 4.0. *Wiley Interdiscip. Rev.: Comput. Mol. Sci.* **2018**, *8*, e1327.
- (81) Neese, F.; Wennmohs, F.; Becker, U.; Riplinger, C. The ORCA quantum chemistry program package. *J. Chem. Phys.* **2020**, *152*.
- (82) Lu, T.; Chen, F. Multiwfn: A multifunctional wavefunction analyzer. *J. Comput. Chem.* **2012**, *33*, 580–592.
- (83) Lu, T. A comprehensive electron wavefunction analysis toolbox for chemists, Multiwfn. J. Chem. Phys. 2024, 161.
- (84) Momma, K.; Izumi, F. VESTA: a three-dimensional visualization system for electronic and structural analysis. *J. Appl. Cryst.* **2008**, *41*, 653–658.
- (85) Fermi, E.; Amaldi, E. *Le orbite [infinito] s degli elementi*; Reale Accademia d'Italia, 1934.